Unsaturated soils: compacted versus reconstituted states

Alessandro Tarantino
Department of Civil Engineering, University of Strathclyde, Glasgow, UK
(formerly Dipartimento di Ingegneria Meccanica e Strutturale, Università degli Studi di Trento, Italy)

ABSTRACT: The paper presents a comparison between compacted and reconstituted soils in terms of microstructure, and hydraulic and mechanical response. It is commonly assumed that reconstituted and compacted soils exhibit a fundamentally different behaviour due to different microstructures. However, the variety of pore size distributions observed in both compacted and reconstituted/natural soils suggests that the boundary between compacted and reconstituted states is more blurred. In the paper, an attempt is made to recognize similarities and differences between compacted and reconstitutes states based on a number of recent experimental studies where the microstructure and the hydraulic and mechanical behaviour of unsaturated soils in compacted and reconstituted states have been investigated. This exercise will also offer the opportunity to gain a better insight into the microstructure of compacted soils.

1 INTRODUCTION

Geotechnical research on unsaturated soils has largely focused on compacted 'double-porosity' geomaterials. When an air-dried soil is moistened, aggregates of clay/silt particles are formed and are generally not destroyed as the soil is statically or dynamically compacted. This results in at least two populations of pores, intra-aggregate pores (within the aggregates) and inter-aggregate pores (between the aggregates) as evidenced by Mercury Intrusion Porosimetry (MIP) tests. In geotechnical engineering, aggregated 'double-porosity' soils generally result from compaction on the dry side of optimum (Ahmed *et al.* 1974, Delage *et al.* 1996). Aggregation also occurs in agricultural soils due to abiotic (freeze-thaw and drying-wetting cycles) and biotic factors (fecal pellets and casts by soil fauna) (Carter 2004).

On the other hand, silty and clayey soils from natural deposits often exhibit a mono-modal Pore Size Distribution (PSD) (e.g. Tanaka et al. 2003), at least in the pore size range investigated by the MIP. The microfabric of geomaterials deposited in water and later exposed either by lowering of the water level or by uplifting of the land can be replicated in the laboratory by reconstituting soils from slurry.

The 'double-porosity' microstructure of soils compacted on the dry side of optimum and the single-porosity microstructure of soils reconstituted from slurry represent two extremes. However, the distinction between single- and double porosity soils is not clear-cut. Soils compacted on the wet side of optimum and having an initial mono-modal pore size distribution may evolve to a bi-modal pore size distribution upon drying (Gens *et al*. 1995, Simms & Yanful 2001). Conversely, soils compacted on the dry-side of optimum and having an initial bi-modal pore size distribution may evolve to a mono-modal pore size distribution upon wetting (Monroy et al. 2010). Similarly, initial bi-modal PSDs in soils compacted on the dry side of optimum may evolve to a mono-modal PSD due to mechanical effects as observed in volumetric collapse upon wetting under loading (Barrera 2002, Gomez *et al.* 2009) or loading at constant suction (Barrera 2002).

On the other hand, reconstituted normally consolidated soils may exhibit a bi-modal pore size distribution at low stresses (Griffiths & Joshi 1989) and a bi-modal pore-size distribution may appear in saturated natural clays in an overconsolidated state (Ninjgarav *et al.* 2007).

It is commonly assumed that reconstituted and compacted soils exhibit a fundamentally different behaviour due to different microstructures. However, if one looks at the variety of pore size distributions in both compacted and reconstituted/natural soils, the boundary between these states is perhaps more blurred. It may therefore be worth comparing the microstructure as well as the macroscopic behaviour of soils in reconstituted and compacted states to identify similarities and differences. A number of experimental studies of hydraulic and mechanical behaviour of soils in both compacted and reconsti-

tuted states have been presented in the literature (Marinho 1994; Jotisinkasa 2005; Monroy 2006; Barrera 2002, Boso 2005, and Buenfil 2007; Tarantino & Tombolato 2005; Tarantino 2009; Koliji 2008) and these will serve as a basis to discuss similarities and differences between compacted and reconstituted states. This comparison will also give the opportunity to gain a better insight into the microstructure of compacted soils.

There is indeed another motivation behind the comparison of compacted and reconstituted states. Many of the concepts developed for unsaturated soils have been established for compacted 'double-porosity' soils. The first generation of unsaturated soil constitutive models formulated in terms of net stress and suction (Alonso et al. 1990, Wheeler & Sivakumar 1995, Cui & Delage 1996) and the second generation of constitutive models that have included the degree of saturation in generalised stress variables (Wheeler et al. 2003, Gallipoli et al. 2003, Tamagnini 2004), have been formulated for and validated against data on double-porosity compacted soils. Similarly, mechanical effects on water retention behaviour have mainly been investigated for compacted double-porosity soils (Vanapalli et al. 1997, Romero et al. 1999, Romero & Vaunat 2000, Gallipoli et al. 2003).

It may therefore be interesting to investigate the aspects of compacted soil behaviour that can be extrapolated to reconstituted/natural unsaturated soils.

2 MICROSTRUCTURE OF COMPACTED SOILS

To prepare compacted samples, air-dried or oven-dried soil powder is sprayed with water to target water contents. Upon spraying, clay particles tend to form aggregates, the size of the aggregates depending on the amount of water sprayed. This is clearly illustrated in Figure 1 which shows aggregates formed after spraying air-dried powder of Speswhite Kaolin to different water contents and then hand-mixing the moistened powder.

At high water contents (w>0.30) very large aggregates formed and, when sieving the moistened powder on the sieve having 1 mm aperture size, about 20-30% of the material was retained on the sieve. The sieved material still had large aggregates as shown in Figure 1a. As water content was decreased to w=0.24, the size of the aggregates forming upon spraying decreased as shown in Figure 1b. At water contents lower than 0.22-0.24, almost all the moistened powder passed through the 1 mm aperture size sieve. Eventually, at very low water content (w=0.10), there was little aggregation as shown in Figure 1c. It is interesting to note that aggregation at very low water contents (w=0.10), as observed by visual inspection, does not seem to significantly differ from that occurring to the kaolin powder under hygroscopic water content w_h as shown in Figure 1d.

The hygroscopic water content is here defined as the water content of the soil in equilibrium with laboratory air at a relative humidity of RH=0.40–0.5. At this relative humidity, water is likely to be adsorbed on clay particles. The thickness δ of the adsorbed water film surrounding the clay particle is related to the hygroscopic gravimetric water content w_h and the specific surface S_a by the following relationship:

$$\delta = \frac{w_h}{S_a \rho_w} \tag{1}$$

where ρ_w is the density of water. On the other hand, the thickness δ can be related to the total suction (chemical potential) of adsorbed water through the following relationship according to Iwamatsu & Horii (1996):

$$\delta = \sqrt[3]{\frac{A_{vsl}}{6\pi\psi}} \tag{2}$$

where ψ is the total suction and A_{svl} is the Hamaker constant, which can be assumed to be equal to 6×10^{-20} J according to Tuller & Or (2005). This relationship only takes into account van der Waals forces on planar surfaces and neglects contribution of capillary condensation, which occurs when adsorbed films on opposing surfaces becomes unstable, grow without bounds and coalesce (Christenson 1994, Tuller *et al*. 1999).

Total suction ψ can be inferred from the measurement of relative humidity of the air in equilibrium with the adsorbed film through the 'psychrometric law' (Tarantino 2010):

$$\psi = -\frac{RT}{v_w}\ln\frac{p_v}{p_{v0}(T)} = -\frac{RT}{v_w}\ln RH \tag{3}$$

where T is the absolute temperature, R is the universal gas constant, v_w is the molar volume of liquid water, p_v is the pressure of the vapour in equilibrium with the liquid, p_{v0} is the saturated vapour pressure at the same temperature, and RH is the relative humidity.

For a relative humidity of RH=0.5, the thickness of the adsorbed film calculated using Eq. (2) and (3) is δ=3.2 Å corresponding to the size of a water molecule. Assuming S_a=14 m^2/g for Speswhite Kaolin according to the technical specification of the supplier, hygroscopic water content w_h=0.0046 is obtained using Eq. (1), which is in excellent agreement with the measured value of w_h=0.005. Banin & Amiel (1970) and Dirksen & Dasberg (1993) also found that hygroscopic water contents in equilibrium with laboratory relative humidity are associated with a monomolecular layer of adsorbed water.

Figure 1d therefore shows the level of aggregation when a monolayer of water molecules envelopes the clay particles. Increasing the water content to w=0.10 (Figure 1c) does not apparently change the level of aggregation. As discussed in the next sections, it is speculated that adding water from hygroscopic water content to w=0.10 does not change the level of aggregation and water only fills the unsaturated intra-aggregate pore space.

When the water content is increased beyond w=0.24 (Figure 1a,b), the added water directly control the size of the aggregates, which are now saturated with water (this point will also be discussed in the next sections). As the compaction water content increases, the size of the aggregates increases. Similar observations have been made by Jotisinkasa (2005) by inspecting thin sections of compacted silty clay

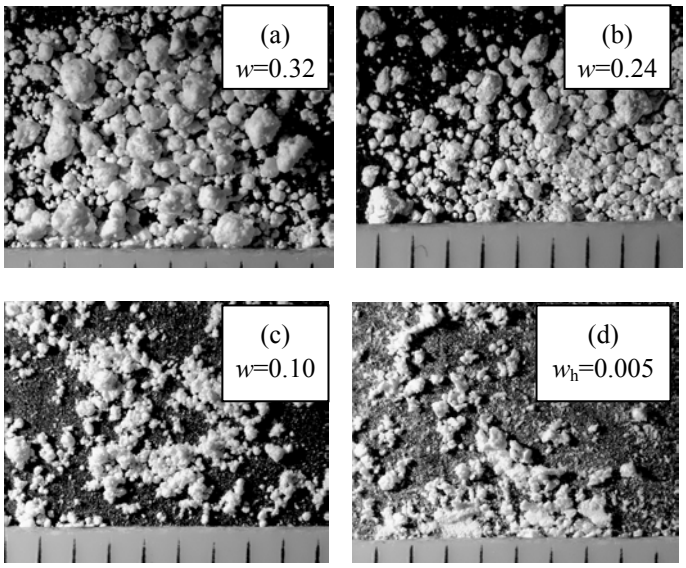

Figure 1. Aggregates forming after spraying Speshwite Kaolin powder with water to different water contents w as observed using an optical microscope (ticks are 1 mm spaced) (Tarantino & De Col 2009)

As the aggregates are placed in the mould for compaction, the inter-aggregates voids are filled with air and water only occupies the intra-aggregate pore space. Pore-water pressure in the aggregates is negative and controlled by the curvature of the menisci at the aggregate boundary. As the soil is loaded (dynamically or statically), the saturated aggregates are subjected to undrained loading, which causes the pore-water pressure in the aggregates to increase (as a first approximation, the saturated aggregates can be assumed to be normally consolidated). If the pore-water pressure remains at values lower than zero (i.e. lower than the pressure of the surrounding air), the aggregates may undergo some distortion but their volume will remain constant. However, if the pore-water pressure tends to increase to values greater than zero, water will be expelled from the aggregates and will invade the inter-aggregate pore-space.

This qualitative representation of the compaction process will serve as basis to discuss the effect of water content, compactive effort and compaction method on microfabric as observed in Mercury Intrusion Porosimetry (MIP) and, to a lesser extent, in the Scanning Electron Microscope (SEM). The MIP investigation is here prioritised as it provides a quantitative assessment of soil microfabric. Since the pioneering work of Diamond (1970, 1971), MIP has been widely used to assess hydraulic and mechanical effects on microstructure in natural and compacted soils (a review of this technique can be found in Romero & Simms 2008).

The technique used for soil dehydration before MIP testing is of great importance to preserve soil microfabric. Standard air-drying has proven to change significantly the pore-size distribution (Ahmed et al. 1974) and the freeze-drying technique (Delage & Pellerin 1984) has therefore become a standard in soil specimen preparation for MIP. This technique consists in rapid freezing the soil in liquid nitrogen or intermediate cooling liquid and subsequent sublimation under vacuum so as to eliminate the formation of air-water menisci that will cause shrinkage on drying. Cooling can be achieved using intermediate cooling liquid like freon (Delage *et al.* 1982; Griffiths & Joshi 1989) or isopentan (Tarantino & De Col 2008). However, cooling of nitrogen down to its freezing point (-210°C) by applying a vacuum appears to be the simplest and most efficient method (Delage *et al.* 2006). In this paper, only MIP results on freeze-dried samples will be discussed.

2.1 *Effect of compaction water content*

Ahmed *et al.* (1974) investigated the effect of compaction water content on the pore-size distribution of Grundite silty clay (index properties summarised in Table 1). Two samples were compacted on the dry side and wet side of optimum at nearly the same void ratio, e=0.80 and e=0.79 respectively. A third sample was compacted at the optimum water content and a lower void ratio was obtained (e=0.73). The results of MIP tests are presented in Figure 2 in terms of cumulative and frequency distribution (original data were processed to derive the frequency distribution shown in Figure 2b).

Data are presented in terms of intrusion volume ratio e_{MIP} defined as the intruded volume $V_{intruded}$ per unit volume of solids, V_s:

$$e_{MIP} = \frac{V_{intruded}}{V_s} \tag{4}$$

In this way, the value e_{MIP} at the end of the intrusion stage can directly be compared with the void ratio e determined in a traditional way by measuring

the volume and water content of the sample from which the specimen for MIP was taken. As shown in Figure 2a, there is a large volume of pores that were not intruded. In this particular case, the maximum pressure applied to mercury was relatively small and a significant amount of intra-aggregate porosity was not intruded. More in general, when the pressure applied to mercury attains the classical 200 MPa, the pores that are not intruded are generally the pores within elementary particle arrangements (inter-particle pores) or intra-particle pores.

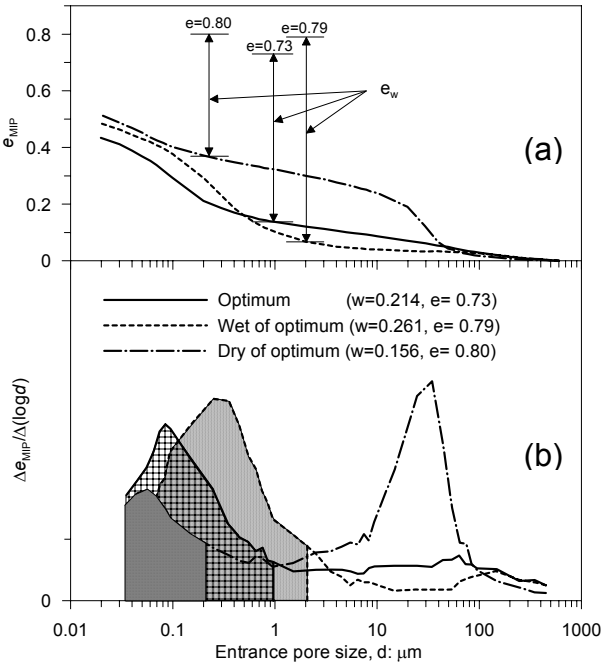

Figure 2. Pore size distribution of Grundite clay compacted at various water contents (a) Cumulative intrusion volume ratio. (b) Intrusion volume ratio frequency (after Ahmed *et al.* 1974).

A schematic representation of microfabric of compacted soils is shown in Figure 3 according to Collins & McGown (1974) and Alonso *et al.* (1987). The basic unit in natural and compacted clayey soils is not the single clay platelet but domains constituted by groups of clay platelets. Intra-domain pores are referred to as *intra-elemental* pores in Figure 3. Domains then group together to form aggregates and pores within the aggregates are referred to as *intra-aggregate* pores. Finally, pores exist between the aggregates and are referred to as *inter-aggregate* pores. In addition to these classes of pores, interlayer pores exist between the elementary layers inside smectite particles (Delage *et al.* 2006). MIP can only detect inter-aggregate and intra-aggregate pores, rarely intra-domain pores, never intra-particle pores.

Figure 2 shows that samples compacted on the dry side of optimum exhibit a bi-modal pore-size distribution whereas samples compacted on the wet side of optimum and at optimum water content essentially exhibit a mono-modal pore-size distribution. Similar observations were made by Delage et al. (1996) and Prapaharan *et al.* (1991) for two other clayey soils.

For the sample compacted on the dry of optimum, the larger modal pore size (~30 μm) represents inter-aggregates pores whereas the smaller modal size (~0.06 μm) represents the intra-aggregate pores (Figure 2b). On the other hand, the sample compacted on the wet side of optimum exhibits a single mode at around 0.3 μm representing intra-aggregate pores. The different fabric of soils compacted on the dry and wet side of optimum is shown in Figure 4 for the Jossigny silt (Cui 1993). On the dry side of optimum aggregates are clearly visible as well as inter-aggregate pores being in the order of tenths of microns. On the other hand, there are no detectable aggregates in the soil compacted on the wet side of optimum and the space between silt particles are filled with the clay fraction that form a relatively uniform matrix.

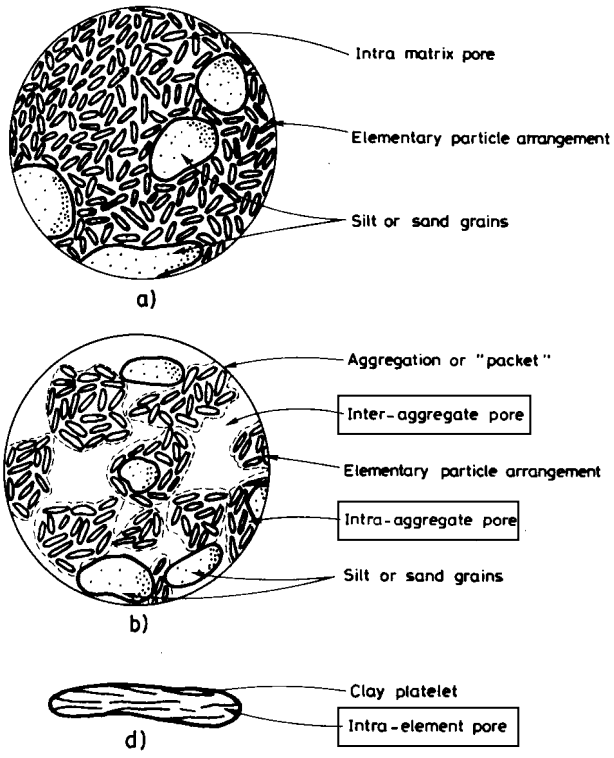

Figure 3. Inter-aggregate, intra-aggregate and intra-domain (intra-element) pores in clayey soils. (a) compacted on the wet side of optimum. (b) compacted on the dry side of optimum. (d) elementary particle arrangement or domain (after Alonso *et al.* 1987).

It is then interesting to visualise the pore space occupied by pore-water. If one assumes that water saturates the smallest pores, the pore entrance size separating the pores filled with water from those filled with air can be can be obtained by subtracting the water ratio e_w to the void ratio e as shown in Figure 2a (water ratio e_w is the volume of water per volume of solids, $e_w=wG_s$). If the pore-water is reported on the frequency pore size distribution, it

clearly appears that water has saturated the aggregates and that the inter-aggregates pores are filled with air. It is interesting to observe that as the compaction water content increases, the modal size of the intra-aggregate pores and their frequency also increases. For example, the modal intra-aggregate pore size increases from 0.05 to 0.08 to 0.3 μm when compaction water content w is increased from 0.156 to 0.214 to 0.261. As shown later in this section, the increase in frequency of the modal intra-aggregate pore size can be explained by considering that the size of the aggregates increases as the compaction water content increases (as shown in Figure 1).

Table 1. Index properties of soils discussed in the paper

Soil	Clay (%)	Silt (%)	Sand (%)	w_p (%)	w_l (%)
Grundite clay *(Ahmed et al. 1974)*	65	35	-	52	22
Jossigny silt *(Delage et al 1996)*	34	56	10	19	37
Silt/kaolin (90/10) *(Garcia-Bengochea et al. 1979)*	8	90	2	N/A	N/A
MX80 Bentonite *(Tang & Cui 2005)*	60	40	-	46	520
Boom Clay *(Romero et al. 1999)*	50	47	3	29	56
Kaolinite *(Shridaran et al. 1971)*	72	28	-	26	62
Speswhite kaolin *(Tarantino & Tombolato 2005)*	80	20	-	32	64
Kaolinite, montmorollonite *(Griffiths & Joshi 1989)*	N/A	N/A	-	30.4	100
Silty sand *(Huang et al. 1994)*	10	37	53	17	22
BCN silt *(Barrera 2002, Boso 2005, Buenfil 2007)*	37	45	18	16	32
Sandy loam *(Cuisinier & Laloui 2004)*	N/A	N/A	N/A	18	30
Clayey silt *(Jotisinkasa et al. 2009)*	27	55	18	18	28
London clay *(Monroy et al. 2010)*	58	40	2	29	83
Glacial till *(Simms & Yanful 2001)*	8	14	18	18	27
Champlain clay *(Delage & Lefebvre 1984)*	80	20	-	25	60
Kaolinite clay *(Hattab et al. 2010)*	59	41	-	20	40

The mono-modal pore size distribution of soils compacted on the wet side of optimum is characteristic of fine-grained soils (as shown in Table 1, Jossigny silt and Grundite clay have a significant clay fraction). This may not be the case of soils having a reduced clay fraction. Garcia-Bengochea *et al.* (1979) tested a mixture consisting of 90% silt and 10% clay and observed a bi-modal pore size distribution even in samples compacted on the wet side of optimum (Figure 5).

In this case, aggregations of clay particles are likely to coat the silt particles or to form bridges between them. The soil skeleton is made of silt grains, which do not expand and fill the large pores as the water content is increased. The large pores observed in the samples compacted on the wet side of optimum and at the optimum water content are perhaps inter-grain pores rather than inter-aggregate pores. Bi-modal pore size distributions of soils compacted on the wet side of optimum were also observed by Simms and Yanful (2001) testing a glacial till, which again included a relatively small clay fraction (Table 1).

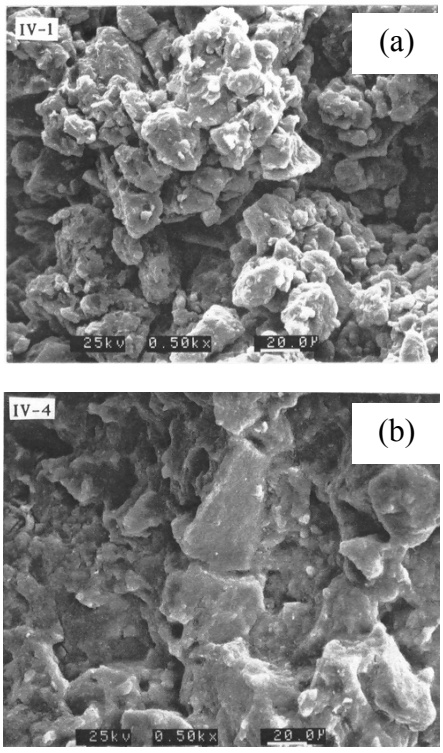

Figure 4. SEM micrographs of Jossigny silt compacted (a) on the dry side of optimum and (b) on the wet side of optimum (Cui 1993).

Inspection of Figure 5 reveals that pore-water fills the aggregates in the sample compacted on the dry side of optimum (similarly to the Grundite clay in Figure 2). In contrast, water also fills the inter-grains pores when the soil is compacted at optimum water content and on the wet side of optimum.

The effect of compaction water content on the PSD of clays compacted on the dry side of optimum was investigated in detail by Tarantino & De Col (2008). Samples with water content ranging between 0.086 and 0.299 were statically compacted to 1200 kPa vertical stress and subsequently tested in the porosimeter (encircled samples in Figure 6). The frequency distribution is shown in Figure 7. Specimens with the higher water content (w=0.299, 0.259, and 0.215) show two modal pore sizes at about 0.1-0.2 and 0.6-0.7 μm. As water content increases, the modal sizes remain unchanged but the intra-aggregate and inter-aggregate porosity redistribute. In particu-

lar, inter-aggregate porosity decreases and intra-aggregate porosity progressively increases as water content increases. Such an evolution of the PSD with water content is very similar to the one observed in Grundite clay (Figure 2). At much lower compaction water contents (w=0.141 and 0.086), the intra-aggregate modal size seems to disappear with a significant increase in the frequency associated with the inter-aggregate modal pore size of 0.7 μm.

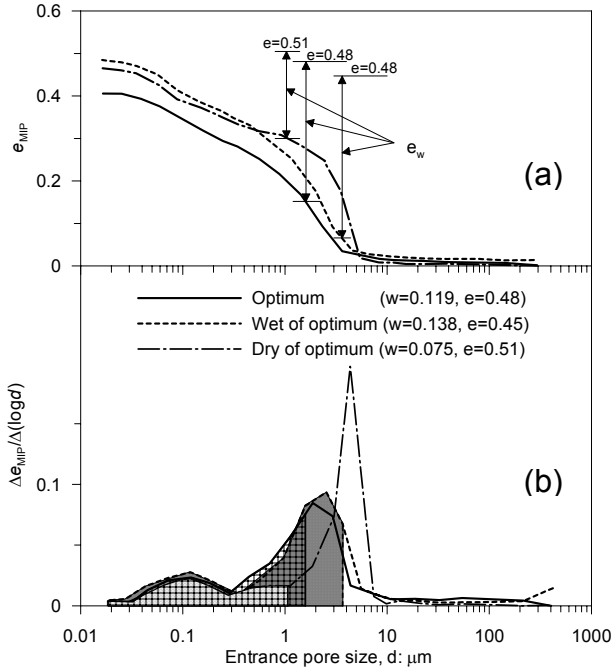

Figure 5. Pore size distribution of Silt/Kaolin (90/10) mixture compacted at various water contents (a) Cumulative intrusion volume. (b) Intrusion volume frequency (after Garcia-Bengochea *et al.* 1979).

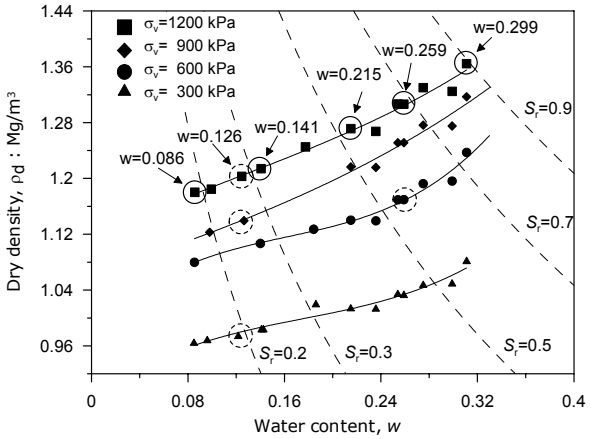

Figure 6. Compaction plane for Speswhite kaolin (after Tarantino and De Col 2008).

The evolution of the PSD with compaction water content presented in Figure 7 is directly related to the size of the aggregates, which increases as water content increases (Figure 1). This effect can be explained by considering a very simple microstructural model. Let us assume that aggregates are formed by domains of clay platelets, represented by circles in Figure 8, and that saturated aggregates are formed when the dry powder is sprayed with water. If the compaction water content is low, aggregates need to be small for the aggregates to be saturated (Figure 8a). As water content is increased, larger aggregates may form still remaining fully saturated (Figure 8b,c).

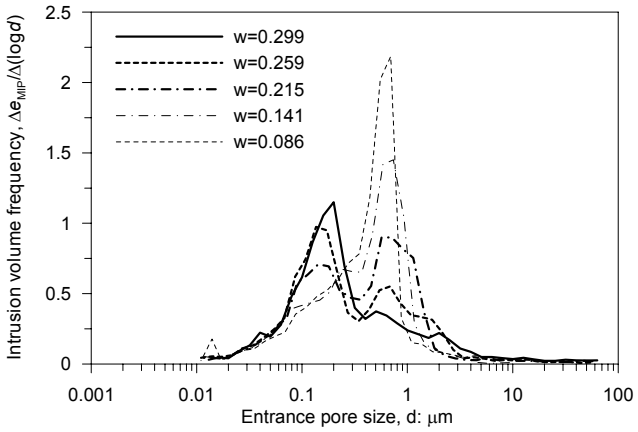

Figure 7. Pore size distribution Speswhite kaolin compacted at various water contents on the dry side of optimum (after Tarantino and De Col 2008).

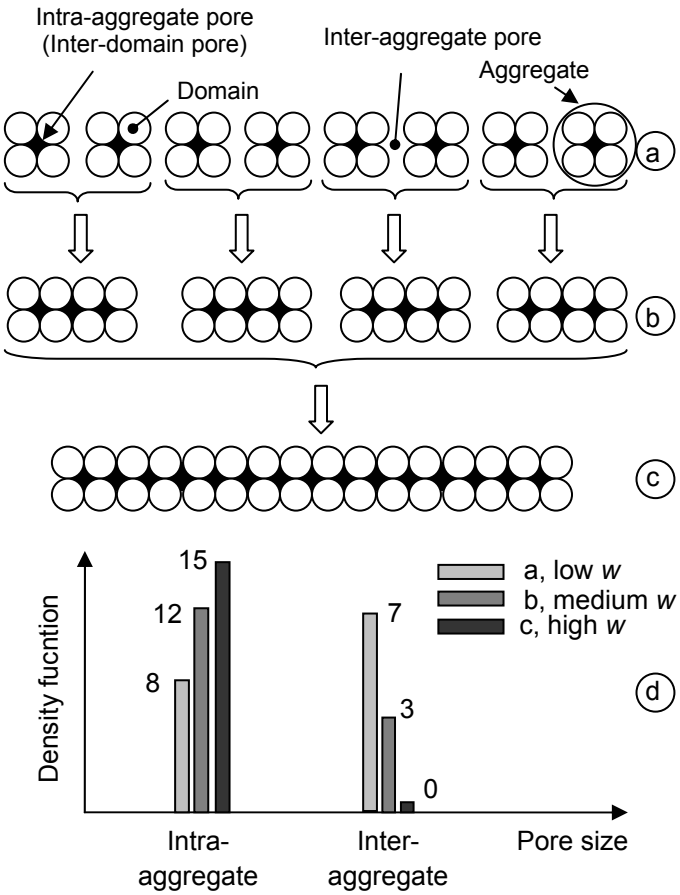

Figure 8. Schematic representation of the relationship between compaction water content and volume of intra- and inter-aggregate pores (black regions represent water).

The density function of such a schematic packing is presented in Figure 8d. As the compaction water content increases, the number of intra-aggregate pores (proportional to the amount of compaction wa-

ter content if the aggregates are assumed to be saturated) increases from 8 to 12 to 15 whereas the number of inter-aggregate pores decreases from 7 to 3 to 0. This evolution of the PSD of this elementary packing is essentially the one observed in Figure 2 and Figure 7.

According to the mechanism presented in Figure 8, the decrease in the frequency associated with the intra-aggregate pore size (~0.2 μm) in the samples compacted at the lower water contents should not be interpreted as the disappearance of aggregates. Indeed, it is associated with a reduction of the aggregate size due to a deficiency in compaction water content.

The mechanism illustrated in Figure 8 would suggest that microfabric of compacted soils in terms of size and number of aggregates is essentially controlled by the compaction water content. To a lesser extent, size and number of aggregates may also be controlled by the procedure used to moisten the soil powder. Experimentalists know well how the process of compaction is operator-dependent.

2.2 *Effect of compactive effort*

The compactive effort controls the dry density of the compacted soils and, hence, its pore size distribution. Delage (2009) reinterpreted PSD data from Shridaran et al. (1971) relative to a kaolinite compacted to different void ratios. He showed that soil compression occurs at the expenses of the macropores, the intra-aggregate porosity remaining essentially unaffected by the overall change in void ratio (Figure 9). Similarly Lloret *et al.* (2003) showed that compaction of bentonite only reduced inter-aggregate porosity whereas intra-aggregate pores remained unaffected.

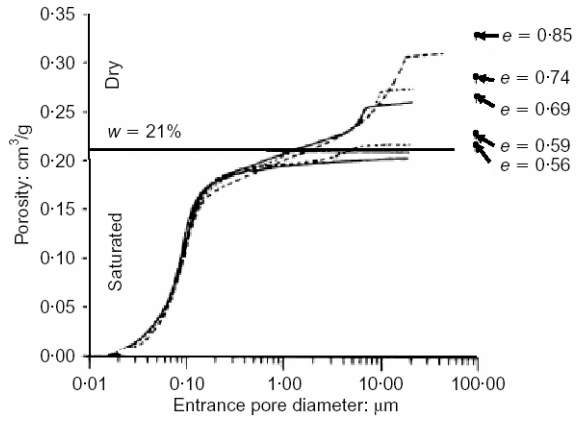

Figure 9. Cumulative pore size distributions of Kaolinite compacted to various densities at same water content (Delage 2009 after Shridaran *et al.* 1971).

Slightly different results have been obtained by Romero et al. (1999) on Boom clay compacted on the dry side of optimum as shown in Figure 10. Similarly to Shridaran *et al.* (1971), the increase in dry density occurs at the expense of inter-aggregate macropores (inter-aggregate modal pore-size decreases from 2000 nm to 600 nm when dry density is increased from 13.7 to 16.7 kN/m^3). However, the intra-aggregate modal pore size also decreases (from 60 to 20 nm) suggesting that compression also affects the arrangement of the aggregates. It is interesting to observe that pore-water (shaded areas in Figure 10b) completely fills the intra-aggregate pore space and seems to slightly invade the macrospores.

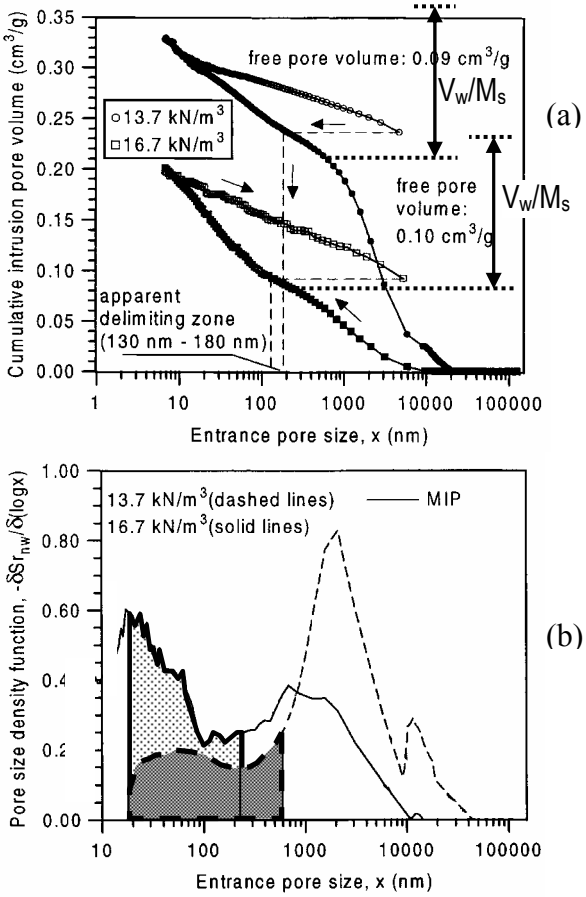

Figure 10. Pore size distribution of Boom Clay compacted at w=15% at different dry densities (a) Cumulative intrusion volume. (b) Intrusion volume frequency (Romero *et al.* 1999).

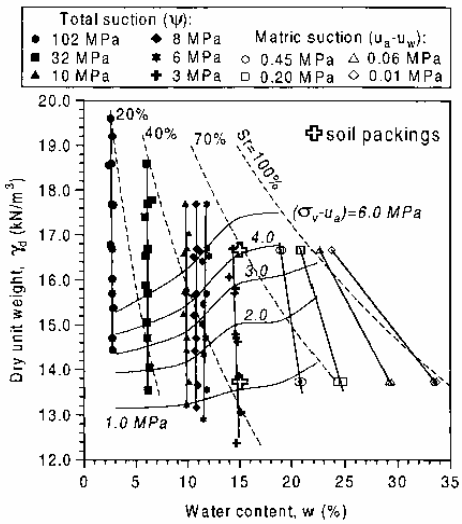

Figure 11. Compaction plane and contours of iso-suction (post-compaction) of Boom clay (Romero *et al.* 1999).

It can be inferred that compression of the saturated aggregates have increased pore-water pressure within the aggregate to values greater than zero causing water to be expelled form the aggregates with the consequent reduction of the aggregate size. The fact that water only slightly invaded the macropores implies that suction was not affected by the change in the macropores (inter-aggregate pores) as confirmed by the vertical contours of equal suction in Figure 11 (crosses in Figure 10 at w=15% represents the as-compacted states investigated). It can be speculated that further compression would have caused more water to be expelled from the aggregates and the suction would eventually be affected by compression of the macropores. The contours of equal suction would have therefore been expected to deviate on the left side as shown by Li (1995, quoted by Delage & Graham 1995).

The effect of compaction effort on pore size distribution is also shown in Figure 12 for compacted Speswhite Kaolin (specimens tested in the MIP are dashed-encircled in Figure 6). At relatively high water content (w=0.259), compression occurs again at the expenses of inter-aggregate pores (modal size ~0.7 μm) with a very slight compression of the intra-aggregate pores).

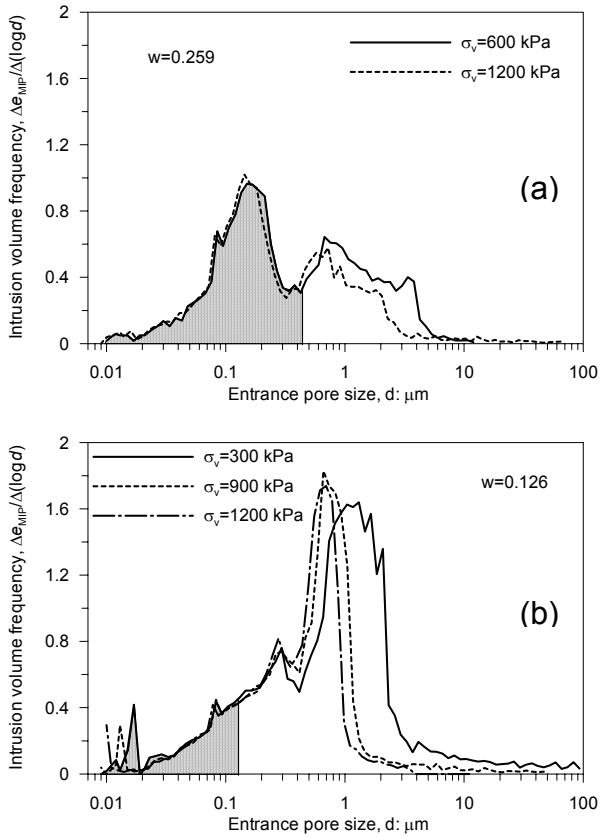

Figure 12. Pore size distribution Speswhite kaolin compacted to different vertical stresses at constant water content (Tarantino, in prep.,a)

It is worth observing that pore-water (grey shaded area) fills the intra-aggregate pores and partly invades the macropores. It is therefore not surprising that irreversible compression of the macropores associated with the increase in vertical stress from 600 to 1200 kPa causes a change in suction in the post-compacted samples.

This is illustrated in Figure 13 where the relationship between suction and degree of saturation during the compaction process of samples having different water contents is presented (Tarantino & De Col 2008). Samples were statically compacted at constant water content under one-dimensional conditions by applying loading-unloading cycles to 300, 600, 900, and 1200 kPa. The dashed lines join the unloaded states often referred to 'as-compacted states'. For the sample having water content w=0.259, the suction after unloading from 600 kPa (open circle) is different from the suction recorded after unloading from 1200 kPa (solid circle), confirming that an irreversible change in the inter-aggregate porosity causes an irreversible change in suction when pore-water occupies the inter-aggregate pore-space. The fact that post-compaction suction increases with the degree of saturation, which is not intuitive at first sight, has been demonstrated to be due to the effect of void ratio on the water retention curve (Tarantino & De Col 2008).

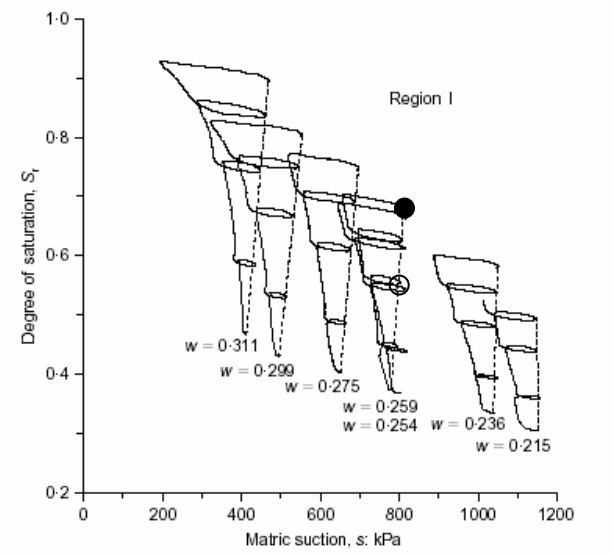

Figure 13. Degree of saturation–suction paths at different compaction water contents. Dotted lines join 'post-compaction' suction (Tarantino and De Col 2008).

The evolution of PSD of a sample compacted to vertical stresses of 300, 900, and 1200 kPa at a significantly lower water content (w=0.126) is shown in Figure 12b. It is again observed that volume reduction occurs at the expenses of large inter-aggregate macro-pores. However, two aspects that have not been observed in any of the PSDs previously shown are worth noticing. The intra-aggregate pore space now appears to be unsaturated (the amount of water present in the micropores is represented by the grey shaded area). It will be shown later on in the paper that the partial saturation of the aggregates can be

associated with the partial saturation of the same soil in a reconstituted state at the same water content. This demonstrates that the common assumption that aggregates in compacted soils are saturated, although often correct, does not always hold.

Since pore-water has withdrawn within the aggregates, irreversible changes in the macropores (inter-aggregates pores) should not cause any change in suction. This is indeed the case for the sample compacted at the water content of w=0.126 as shown by the vertical contours of equal post-compaction suction in Fig. 10 of the paper by Tarantino & De Col (2008). This is also the case of the sample compacted at the water content of w= 0.215 in Figure 13 as the dashed line joining the post-compaction states appears to be vertical. Nonetheless, for this sample, suction decreases during loading presumably because of the elastic water-undrained compression of the aggregates.

The second interesting aspect is the modal size appearing in the sample at low water content in the range 0.01-0.02 μm. In particular, this modal size shifts from 0.017 μm at σ_v=300 kPa to 0.01 μm at σ_v=1200 kPa. These pores may be inter-particle (intra-domain) pores whereas the modal size in the range 0.1-0.2 mm characterising the intra-aggregate size (Figure 12a) may be associated to inter-domain pores (this point will be discussed further on).

2.3 *Effects of compaction method*

A question that is worth addressing is the difference between static, dynamic and kneading compaction. Static compaction is often used in the laboratory to control the stress history of samples subsequently subjected to mechanical testing. However, kneading and dynamic compaction are more representative of field compaction.

Ahmed *at al.* (1974) presented PSDs of Grundite clay compacted on the dry and wet side of optimum and at optimum water content using dynamic, kneading and static compaction. Figure 14 shows the PSDs of samples compacted on the dry side of optimum at the same dry density and using different compaction methods.

No significant differences were observed and similar results were obtained for samples compacted on the wet side of optimum and at the optimum water content. Prapaharan *et al.* (1991) compacted medium plastic clay (w_l=38%, w_p= 16%) using dynamic (impact) and kneading compaction. Some minor differences where only observed for the samples compacted on the dry side of optimum in the range of inter-aggregate porosity.

The compaction method does not appear to have any effect on the PSD of compacted soils. As suggested in Figure 8, the size and number of the aggregates would mainly depend on the compaction water content. Data shown in Figure 14 would suggest that the process of compaction does not break the aggregates and, hence, different compaction methods do not alter the microstructure.

The negligible effect of the compaction method on the soil microstructure seems to be corroborated by the results obtained by Wheeler & Sivakumar (2000) who tested kaolin samples statically and dynamically compacted to the same dry density and found no appreciable differences in terms of stress-strain response in the triaxial apparatus.

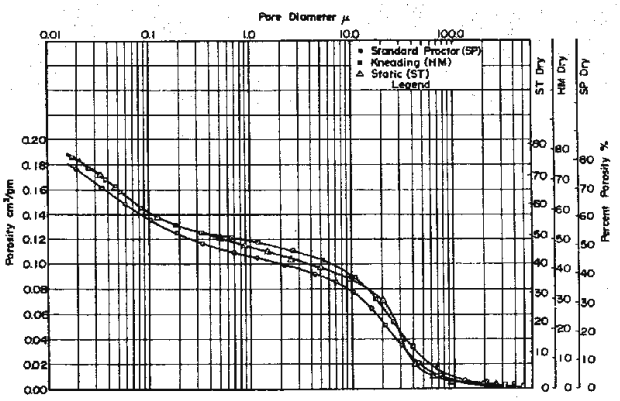

Figure 14. Pore size distributions for compaction on dry side by different compaction methods (Ahmed *et al.* 1974).

It should be noted that the comparison presented in Figure 14 concerns samples compacted in the laboratory. Differences arise when comparing PSD of samples compacted in the field and in the laboratory. Jommi & Sciotti (2003) compared the PSD of a soil taken from a compacted embankment and the one obtained in the laboratory after the borrow soil was initially dried, passed through the sieve No. 200, mixed to the target water content with tap water, cured and dynamically compacted to similar dry density as in the field.

The comparison is shown in Figure 15 and it can be observed that differences, at least in terms of PSD, essentially occur in the range of inter-aggregate porosity whereas the intra-aggregate porosity is similar as also inferred from the similar non-constricted porosity as detected by mercury extrusion (Jommi & Sciotti 2003). This is remarkable as the soil in the field is compacted in peds, which are likely to retain the same structure of the natural soil. On the other hand, the soils compacted in the laboratory was crushed, sieved, and wetted again.

3 MICROSTRUCTURE OF RECONSTITUTED SOILS

There are few data on PSD of reconstituted soils in unsaturated state. Speswhite Kaolin reconstituted from slurry and subsequently air-dried was tested at the University of Trento. The drying curves in terms

of void ratio e, water ratio e_w, and degree of saturation S_r are reported in Figure 16.

For suctions lower than around 800 kPa, the slurry remained saturated and the soil followed the saturated normal consolidation line. As the soil desaturated, the void ratio rapidly attained a nearly constant value whereas the water ratio and the degree of saturation kept decreasing. Two saturated and two unsaturated samples (encircled in Figure 16) were tested using MIP as shown in Figure 17. The PSD distribution is mono-modal with modal size around 0.2 μm. This modal size is essentially the same as the intra-aggregate modal pore size of the same soil in compacted state (Figure 7).

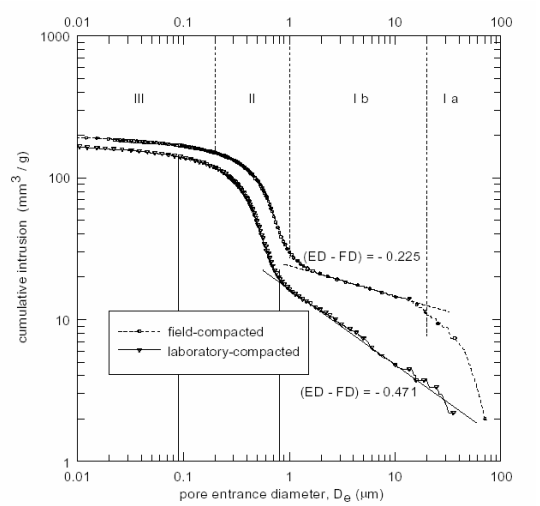

Figure 15. Log-log representation of cumulative intrusion curve of field and laboratory compacted samples (Jommi & Sciotti 2003).

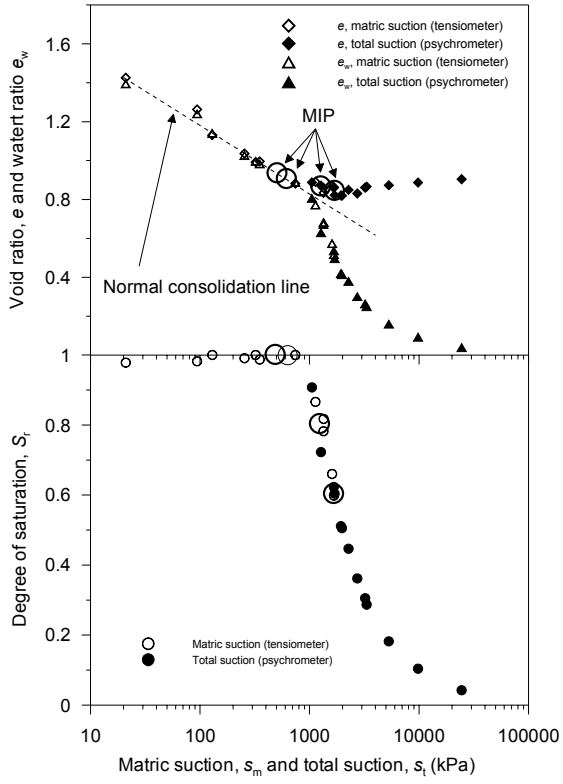

Figure 16. Free-drying behaviour of Speshwite kaolin prepared from slurry at 1.5 w_l (Tarantino, in prep., b).

It is interesting to notice that the modal pore size decrease when the water ratio decreases from 0.934 to 0.901 to 0.720 and then shifts back to a higher value at the lower water ratio (e_w=0.495). This is associated to the slight increase in void ratio as the soil desaturates (Figure 16).

Figure 18 shows the PSD of two reconstituted samples of Bioley silt (Koliji *et al.* 2010). One sample (PR2) was loaded under saturated conditions and the other one (PR1) was dried to a suction of 500 kPa under a total vertical stress of 500 kPa. Again, the pore size distribution remains mono-modal under the combined effect of loading and suction.

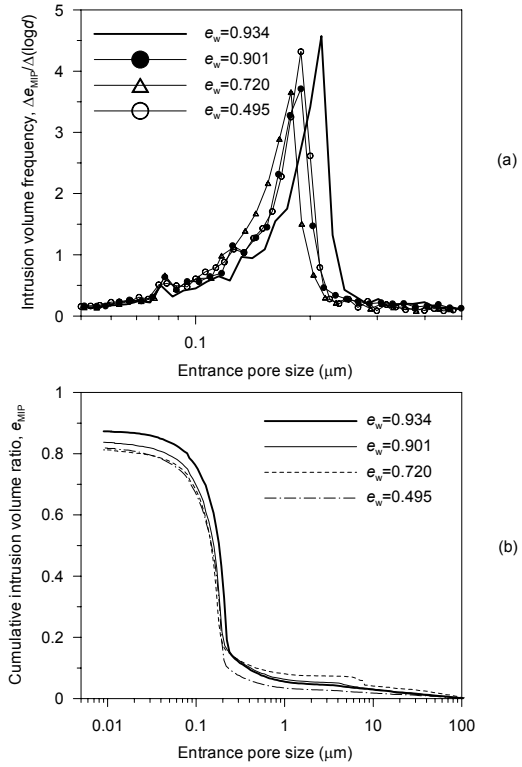

Figure 17. PSDs of Speshwite kaolin prepared from slurry at 1.5 w_l and desaturated by air-drying (Tarantino, in prep., b).

It may be instructive to compare the PSD of these unsaturated reconstituted soils with the PSD of other reconstituted saturated clays. Delage & Lefebvre (1984) measured the PSD of a remoulded saturated Champlain clay (this clay shows similar grain size distribution and consistency limits as indicated in Table 1). They observed that the PSD is mono-modal even if the microstructure consists of aggregates dividing porosity into inter- and intra-aggregate pores as shown by scanning electron microscopy. Similarly, Hattab *et al.* (2010) showed that reconstituted kaolinite essentially exhibits a mono-modal pore-size distribution (Figure 19) even if aggregates can clearly be distinguished using the scanning electron microscope. It is interesting to note that the modal size of 0.182 μm of the reconstituted kaolinite consolidated to 120 kPa vertical stress in Figure 19 is classified as inter-aggregate porosity by Hattab *et al.* (2010). This modal size is very close to

the modal size of reconstituted Speswhite Kaolin as shown in Figure 17, which is in turn very similar to the intra-aggregate size of compacted Speswhite Kaolin as shown in Figure 7.

In other words, the same modal size is classified as inter-aggregate in the reconstituted soil and as intra-aggregate in the compacted soil. This leads to the conclusions that aggregates in compacted clays are made of sub-aggregates (elementary particle arrangements according), which were referred to as aggregates in the reconstituted soil investigated by Hattab *et al.* (2010).

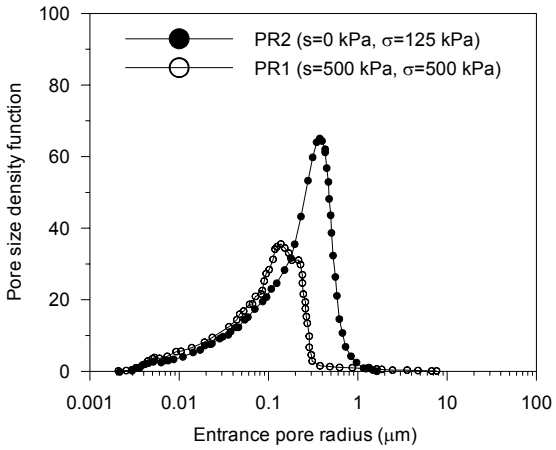

Figure 18. PSD of remoulded Bioley silt at zero suction (PR2) and and after imposing a suction of 500 kPa and a vertical stress of 500 kPa (PR1) (after Koliji *et al.* 2010).

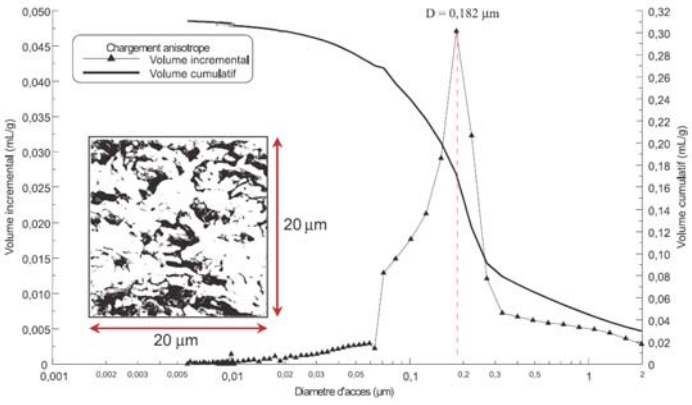

Figure 19. Pore size distribution of reconstituted kaolinite consolidated to 120 kPa vertical stress (Hattab *et al.* 2010).

A question that might be asked is why the pore size distribution of reconstituted soil appears to be mono-modal despite the existence of aggregates whereas the existence of (macro) aggregates in compacted soils is clearly evidenced by a bi-modal pore size distribution. A possible explanation can be provided by inspecting the PSD measured by Griffiths & Joshi (1989) on Kaolinite-Montmorillonite prepared at the liquid limit and subsequently loaded to different vertical stresses. At the liquid limit, two inflection points can be clearly distinguished, which should correspond to intra- and inter-aggregate porosity (Figure 20). However, the inter-aggregate porosity tends to collapse as the soil is loaded. As intra-aggregate and inter-aggregate porosity are of the same order of magnitude, it becomes difficult to distinguish these two classes of pores and the PSD appears to have a single inflection.

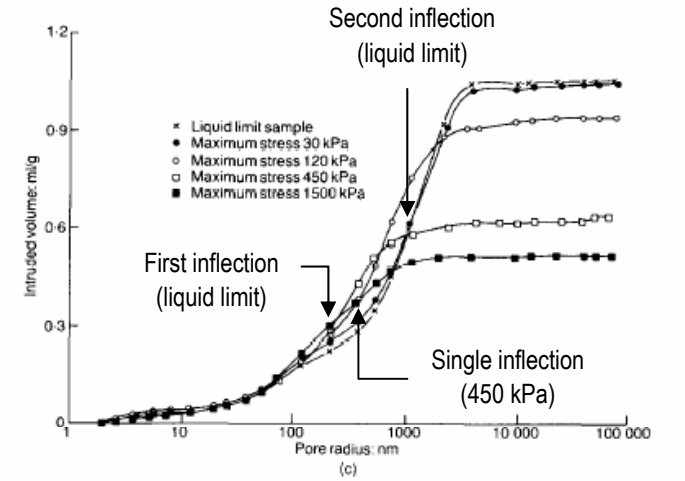

Figure 20. Cumulative pore size distributions of Kaolinite-Montmorillonite prepared at w_l and loaded under saturated conditions (after Griffiths & Joshi 1989).

4 EFFECTS OF WATER CONTENT CHANGE ON MICROSTRUCTURE

4.1 *Changes in microstructure upon saturation*

The pore size distribution generated by the compaction process does not remain unchanged as the soil is subjected to drying or wetting. Monroy et al. (2010) investigated the evolution of the PSD of London clay compacted on the dry side of optimum and then progressively wetted until saturation in a suction-controlled osmotic oedometer. The evolution of the PSD is shown in Figure 21 and shows that intra-aggregate porosity progressively increases in terms of both modal size and frequency until the inter-aggregate porosity is almost entirely erased (Figure 21e). It is interesting to note that there are similarities between the evolution of the PSDs of compacted London clay as it is progressively wetted and the evolution of PSDs of Speshwite Kaolin compacted at different water contents (Figure 7). In both cases, inter-aggregate porosity tends to disappear as water content increases. The only difference lies in the swelling of London clay aggregates probably associated with the smectite fraction of the clay. Figure 21 also shows that the aggregated fabric is not completely erased by hydration and this was confirmed by comparing ESEM photographs of compacted and subsequently hydrated samples and of reconstituted saturated samples (Monroy 2006).

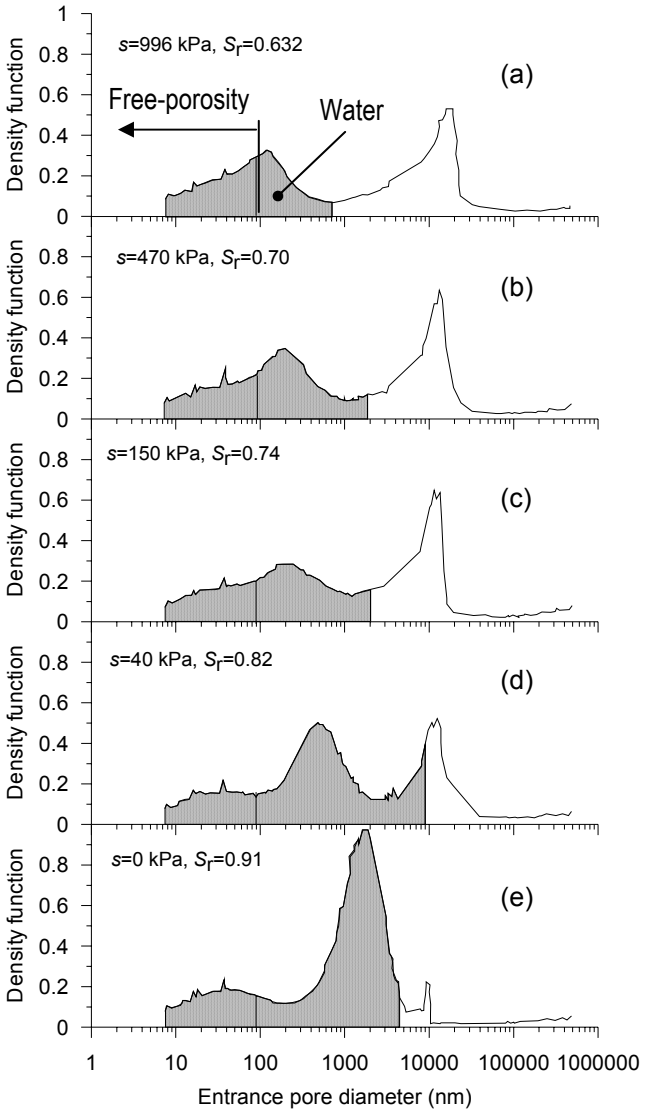

Figure 21. Evolution of pore size distributions of compacted London clay upon wetting (after Monroy 2006, Monroy *et al.* 2010).

Similar conclusions were drawn by Thom *et al.* (2007) on the basis of PSDs determined before and after saturation although some concerns arise from their data as porosimeter data shows a decrease in mercury intruded pore volume upon saturation whereas an overall swelling was observed at macroscopic level upon saturation.

4.2 *Changes in microstructure upon drying*

Cuisinier & Laloui (2004) investigated the evolution of PSD upon drying of a sandy loam compacted on the dry side of optimum, saturated and finally desaturated in the pressure plate. Figure 22 shows the drying curve in terms of void ratio and water ratio (void ratio was calculated from MIP data and corrected for the fraction of pores not intruded by mercury calculated at saturation). As suction is increased from 0 to 200 kPa, the inter-aggregate porosity significantly decreases and the intra-aggregate porosity progressively increases even if the total porosity remains essentially unchanged (Figure 23). When suction is increased from 200 to 400 kPa the inter-aggregate porosity seems to increase again but no higher suctions were applied and it is therefore difficult to understand whether this is simply an experimental error.

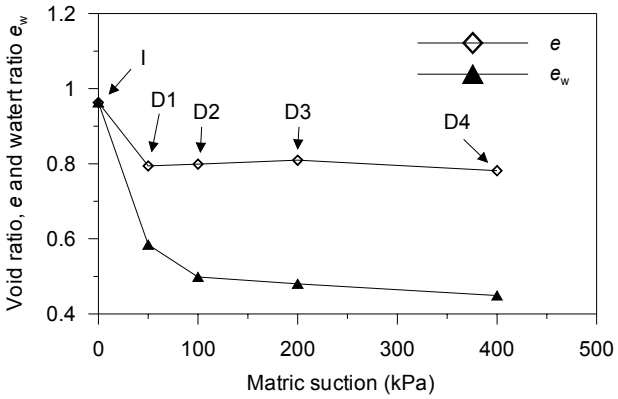

Figure 22. Evolution of water ratio and void ratio (estimated from MIP data) of compacted sandy loam upon drying (after Cuisinier & Laloui 2004).

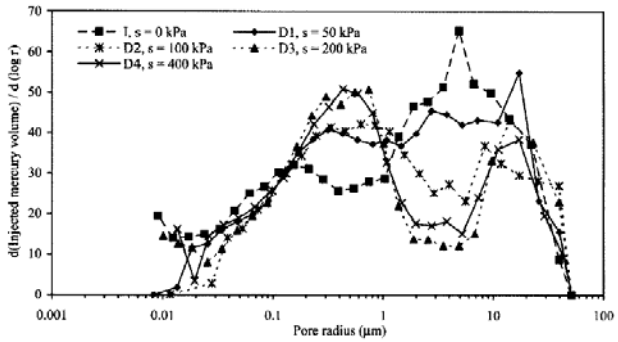

Figure 23. Evolution of pore size distributions of compacted sandy loam upon drying (Cuisinier & Laloui 2004).

The evolution of PSD upon drying was also investigated by Simms & Yanful (2001) by testing a glacial till compacted on the wet side of optimum (the drying curves in terms of void ratio and water ratio are shown in Figure 24). Similarly to Cuisinier & Laloui (2004), the drying process tends to erase the macropores (capillary suction causes the larger pores to shrink) and eventually the initial bi-modal pore-size distribution transformed into a mono-modal pore-size distribution (Figure 25). However, when the soil was air-dried after applying a suction of 2500 kPa (Figure 26), inter-aggregates appeared again, probably due to the elastic rebound of pores that desaturated (desaturation causes a release of the capillary stress). Again, the significant change in pore size distribution upon air-drying shown in Figure 26 occurred at nearly constant overall void ratio.

These MIP data shows that there is not always a direct relationship between microscopic and macroscopic behaviour (e.g. PSD may change significantly at constant void ratio) and that it is difficult to clas-

sify a soil as a double-porosity or double-structure geomaterials as the PSD evolves during hydraulic and mechanical loading.

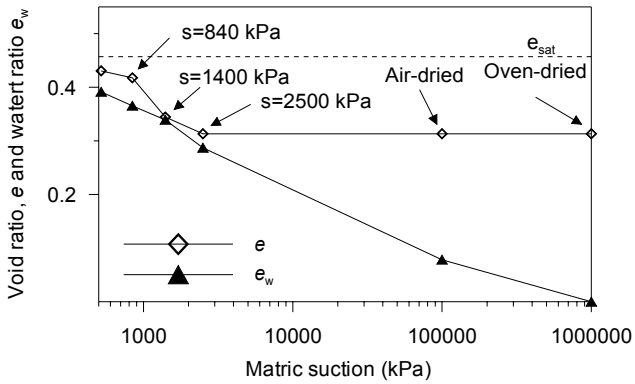

Figure 24. Evolution of water ratio and void ratio (estimated from MIP data) of compacted glacial till upon drying (after Simms & Yanful 2001).

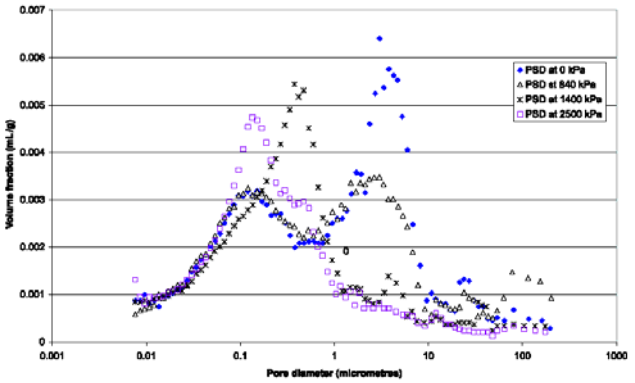

Figure 25. Evolution of pore size distributions of compacted glacial till upon drying (Simms & Yanful 2001).

5 SOIL MICROSTRUCTURE: COMPACTED VERSUS RECONSTITUTED STATES

The variety of pore size distributions in both compacted and reconstituted soils has shown that the boundary between compacted and reconstituted states is blurred. At this point, it may therefore be worth comparing the microstructure of reconstituted and compacted states in terms of pore size distribution. Figure 27 compares the PSDs of Speswhite Kaolin (i) statically compacted to 1200 kPa and (ii) reconstituted from slurry and subsequently air-dried. The comparison is made by considering similar suction levels. It clearly appears that the reconstituted soil exhibits the same modal size as the intra-aggregate modal size of the compacted soil. This leads to the simple conclusion that aggregates are made of reconstituted soil and this appears to be the link between reconstituted and compacted soils.

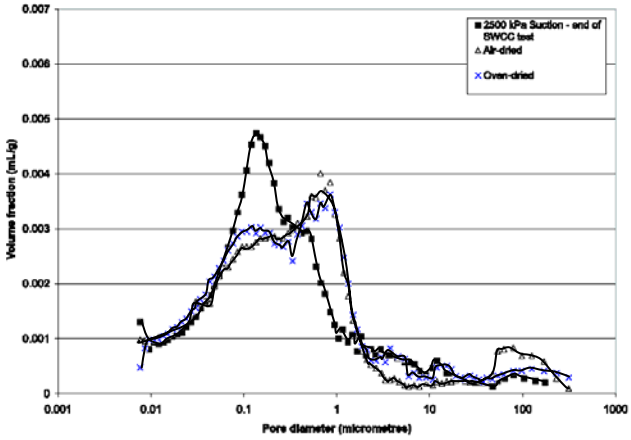

Figure 26. Evolution of pore size distributions of compacted glacial till upon air- and oven-drying (Simms & Yanful 2001).

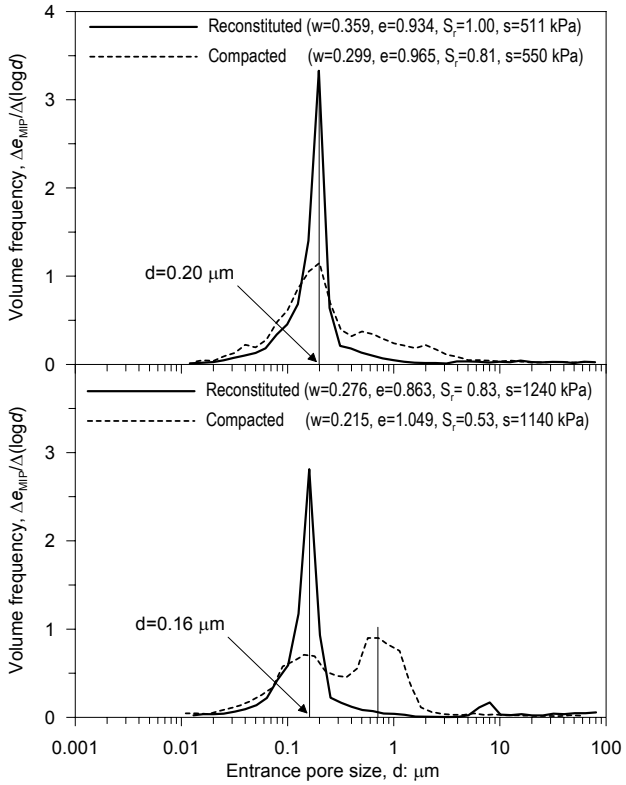

Figure 27. Comparison of PSD of compacted and reconstituted samples of Speswhite kaolin at similar suction (Tarantino, in prep. b).

A similar conclusion can be drawn by comparing the PSD of Barcelona red clay in compacted and reconstituted states. Figure 28 shows the PSD of two samples reconstituted from slurry at 1.5 w_l and consolidated to 100 kPa vertical stress. The first sample was tested immediately after removal from the consolidometer (s=0 kPa) and the second one was air-dried to a suction s=120 kPa (Boso 2005). The other two samples were compacted to different void ratios (e=0.82 and e=0.55) at the same water content of 12% and had a suction of 270 kPa as measured by a high-capacity tensiometer (Buenfil 2007).

The reconstituted samples show mono-modal PSD with modal size that decreases when suction is

increased from 0 to 120 kPa and void ratio is decreased from 0.648 to 0.453. No MIP tests were performed on reconstituted samples at higher suctions but it is reasonable to expect that the modal size would further reduce upon drying.

On the other hand, the two compacted samples exhibit a bi-modal pore size distribution with only the inter-aggregate pores affected by compaction. The modal size characterising the intra-aggregate porosity (~0.4μm) is only slightly smaller than the modal size of the reconstituted sample at s=120 kPa and this difference is likely to be due to the different suction level (270 kPa for the compacted sample against 120 kPa for the reconstituted sample). Again, it would seem that aggregates are made of reconstituted soil.

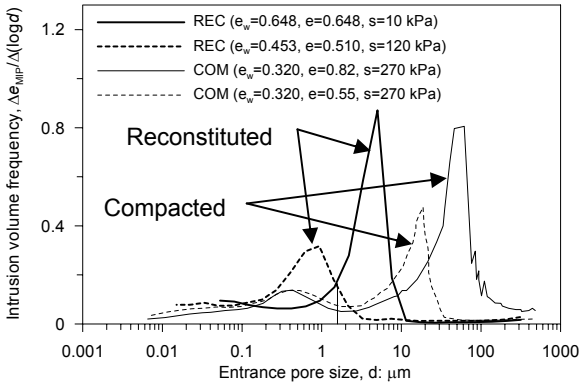

Figure 28. Comparison of PSD of compacted and reconstituted Barcelona red clayey silt (after Boso 2005 and Buenfil 2007).

A similar conclusion can also be drawn from MIP data on compacted and reconstituted samples of Bioley silt (Koliji *et al.* 2010). Compacted samples were prepared by compacting the soil on the dry side of optimum, which was then gently crushed and sieved. Aggregates were oven-dried and then wetted to w=13% using the procedure described by Koliji (2008). Reconstituted samples were prepared by mixing the soil powder to a water content slightly lower than the liquid limit.

Figure 29 compares the PSD of compacted (PS) and reconstituted (PR) samples of Bioley silt at zero suction (PR2 and PS3) and at a suction of 500 kPa and a vertical stress of 500 kPa (PR1 and PS1b). Again, the modal size of the mono-modal pore-size distribution of the reconstituted sample appears to be very similar to the intra-aggregate modal size of the compacted sample.

In the light of these findings, it is not surprising that the field- and laboratory-compacted samples in Figure 15 exhibited the same intra-aggregate porosity. Aggregates forming upon water spraying in the laboratory have a 'reconstituted' structure which is likely to be very similar to natural clay used as construction material.

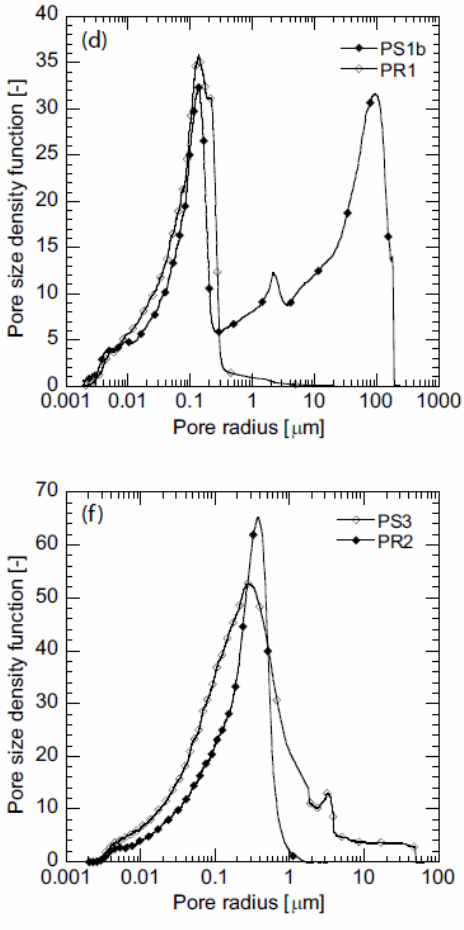

Figure 29. Comparison of PSD of compacted (PS) and reconstituted (PR) samples of Bioley silt at zero suction (PR2 and PS3) and a suction of 500 kPa and a vertical stress of 500 kPa (PR1 and PS1b) (after Koliji *et al.* 2010).

6 RESPONSE UNDER SATURATED CONDITIONS

A first comparison between soils in compacted and reconstituted states can be made by considering the response under saturated conditions. Pore size distribution data of samples compacted and then fully hydrated seem to suggest that the aggregated structure of compacted soils is not destroyed by hydration. It would therefore be expected that some differences occur in the mechanical response of compacted (aggregated) soils and reconstituted soils, where aggregation occurs only at the level of elementary particle assemblages.

Tarantino & Tombolato (2005) compare the direct shear strength of compacted and reconstituted samples of Kaolin Speswhite. Six specimens were statically compacted at different values of vertical stress and water content and then sheared in the direct shear box. Reconstituted specimens were first consolidated to 100 kPa vertical stress in the consolidometer. Specimens were then cut and trimmed from the cake and sheared in the direct shear box at different vertical stresses. The results from these tests are shown in Figure 30, where the ultimate

shear stress τ and the ultimate void ratio *e* are plotted against the effective vertical stress σ'. The ultimate shear strength of the compacted specimens appears to be independent of the compaction conditions, as all data lies on the same curve. Ultimate shear strength data from reconstituted specimens appear to fall on the same envelope defined by the compacted specimens. In addition, the relationship between the void ratio *e* and the vertical stress σ' at failure also appear to be the same regardless of whether the soil was reconstituted or compacted (the void ratio was determined by taking a mass of soil from the shear surface at the end of the test).

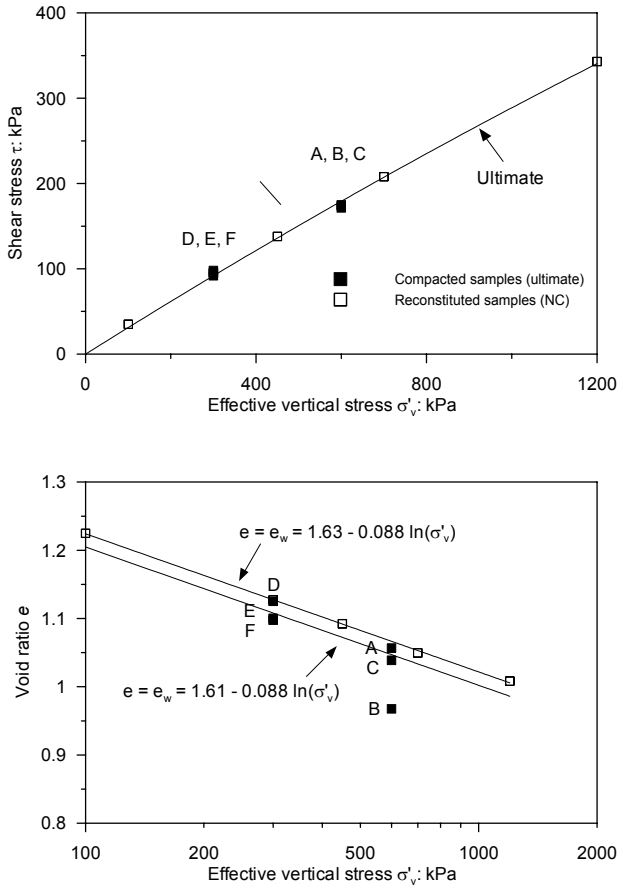

Figure 30. Direct shear data on saturated compacted samples and reconstituted normally consolidated samples of Speswhite kaolin (after Tarantino & Tombolato 2005).

The process of saturation has probably caused aggregates to swell with a reduction of the inter-aggregate space in the compacted samples. This has been probably further reduced by shearing (all samples exhibited contractile behaviour). The microstructure of the compacted soil made by a closed packing of 'reconstituted' aggregates would therefore not be very different from the microstructure of the reconstituted soil. This would explain the same response of compacted and reconstituted soils upon shearing.

Jotisinkasa et al. (2009) tested a mixture of 70% silt, 20& kaolin and 10% London clay in compacted and reconstituted states. Again, in terms of ultimate shear strength there seems to be no difference between reconstituted and compacted samples, TR and TC respectively in Figure 31. Differences appear in the volumetric plane as the critical state line for the compacted soil lies below the one relative to the reconstituted states (Figure 31b).

Differently from the Speswhite Kaolin, the mixture tested by Jotisinkasa *et al.* (2009) contains a significant silt fraction which appears to control the shear strength of the mixture (the critical state friction angle of 32.7° is clearly characteristic of a silt and not of a clay). The fabric of the reconstituted soil observed from thin sections appears to be a uniform matrix of silt and clay particles. On the other hand, the compacted soil exhibits a microstructure where aggregates interact with silt grains (Jotisinkasa 2005). Upon shearing, this microstructure cannot reverse to the uniform matrix of the reconstituted soil and this is perhaps the reason why the critical state lines of the compacted and reconstituted soils appear to be different.

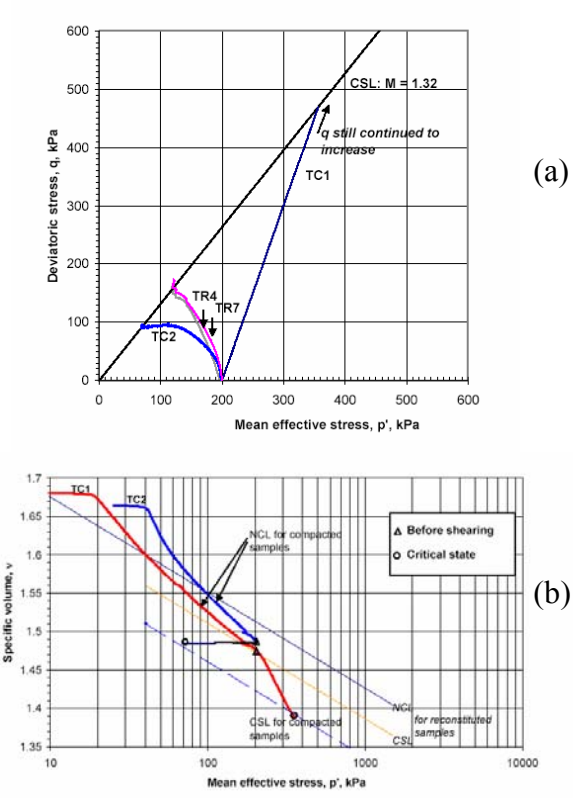

Figure 31. Triaxial data on saturated compacted samples and reconstituted samples of a clayey silt (Jotisinkasa 2005, Jotisinkasa *et al.* 2009).

In terms of compression behaviour, Figure 32 compares the virgin compression of reconstituted and compacted Barcelona red clayey silt. In particular, isotopic compression data of compacted samples obtained by Buenfil (2007) are compared with oedometer virgin compression data on reconstituted samples obtained by Boso (2005) (it was assumed

k_0=1-sinϕ' to convert the vertical stress to mean effective stress). There is good agreement between the virgin compression data of compacted and reconstituted samples.

Virgin compression behaviour of compacted and reconstituted kaolin under saturated conditions is shown Figure 32. The two virgin compression lines appear to have the same slope but the line relative to the reconstituted state lies above the line associated with the compacted state. It is not clear if this is a fundamental difference or it is simply associated with the error in the estimate of the absolute void ratio (tests were carried out in different oedometers and the reference void ratio was estimated in different ways).

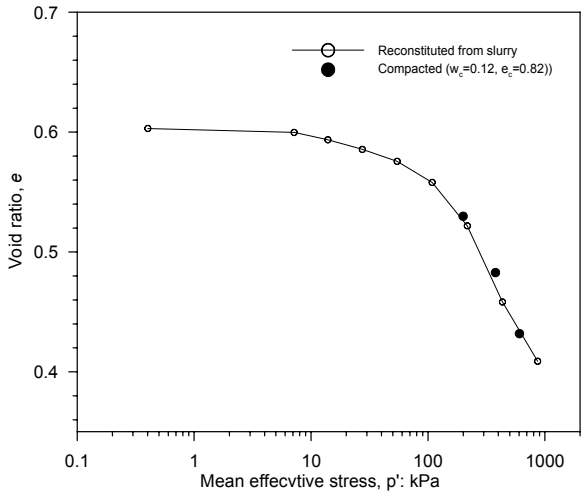

Figure 32. Virgin compression data for reconstituted and compacted Barcelona red clayey silt (after Boso 2005 and Buenfil 2007).

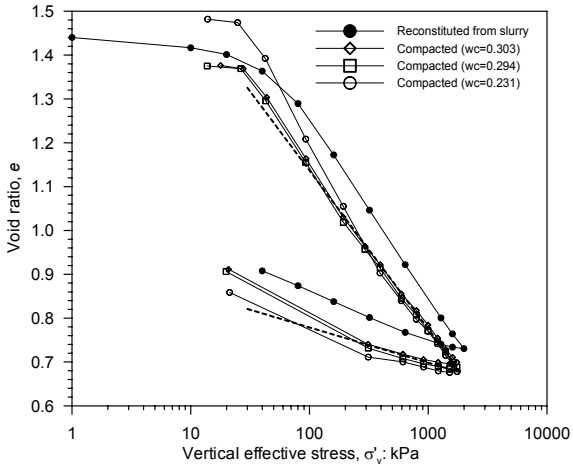

Figure 33. Virgin compression data for reconstituted and compacted Speshwite kaolin (after Tarantino & De Col 2008 and Galvani 2003).

Monroy (2005) also compared the virgin compression behaviour of London clay in reconstituted (*icl*) and compacted samples (*c25*) under saturated conditions. The curve relative to the compacted specimen seems to converge at high stresses to the 'reconstituted' curve. It is however unclear whether the compacted curve tends to become asymptotic with the reconstituted curve at higher stresses or tends to cross it.

From the limited dataset presented in this section, it may be concluded that compacted and reconstituted soils in saturated conditions tend to exhibit the same shear strength. In terms of volumetric behaviour (both virgin compression and critical state), data are not consistent and it is difficult to draw any conclusion in lack of additional data.

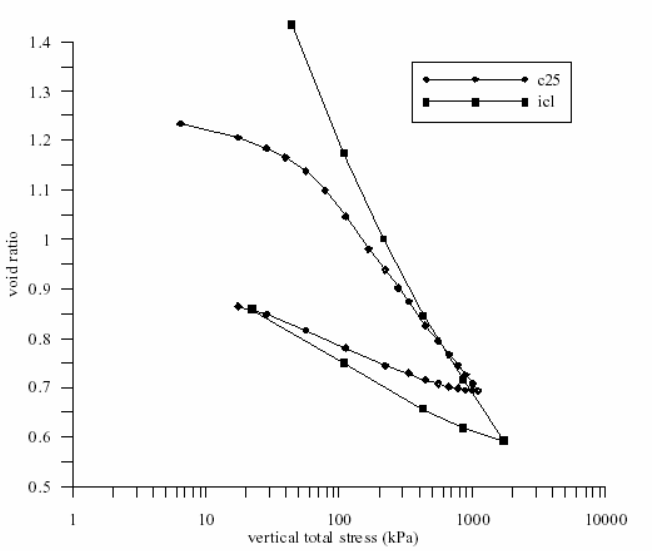

Figure 34. Virgin compression data for reconstituted (*icl*) and compacted fully hydrated (*c25*) London clay (Monroy 2005)

7 WATER RETENTION BEHAVIOUR

The relationship between suction, *s*, and degree of saturation, S_r, or the water content *w*, is referred to as water retention function and plays a key role in the mechanical and hydraulic behaviour of unsaturated soils. The relationships *s*-S_r or *s*-*w* are hysteretic as the response of a soil dried from saturated state ('*main drying*') differs from that of the same soil wetted from dry state ('*main wetting*'). The 'main drying' and 'main wetting' curves mark out the domain of possible attainable states (hysteresis domain). If a saturated soil is dried to an intermediate degree of saturation and is then wetted, the corresponding *s*-S_r curve scans the hysteresis domain, from the main drying towards the main wetting curve, and is therefore referred to as *scanning curve*. The behaviour in the scanning region is often assumed to be reversible, whereas water retention behaviour is irreversible along the main drying and main wetting curve.

Earlier work by Ridely (1993), Huang *et al.* (1998), Vanapalli *et al.* (1999), Karube & Kawai (2001) have shown that the 'main drying' and the 'main wetting' curves for both reconstituted and

compacted soils are void ratio dependent and that main drying and main wetting in deformable soils are then characterised by two surfaces in the space (s, e, S_r) or (s, e, e_w), e being the void ratio and e_w the water ratio. These findings have been later confirmed by Gallipoli *et al*. (2003b), Tarantino and Tombolato (2005), Tarantino (2009), and Salager *et al.* (2010).

Romero *et al.* (1999) were perhaps the first to recognize the interplay between microstructure and water retention behaviour in compacted soils. Figure 35 shows the main drying and main wetting water retention curves at constant void ratio of Boom clay for two dry densities, 13.7 and 16.7 kN/m^3 respectively. For water contents greater than 15%, the main drying and main wetting curves depend on void ratio, with the air-entry suction increasing as the dry density increases. In the range of water contents between 5% and 15%, the main drying and main wetting cease to depend on dry density although hysteretic effects have not vanished. Below the water content of 5%, the relationship between suction and water content becomes independent of the direction of the hydraulic path.

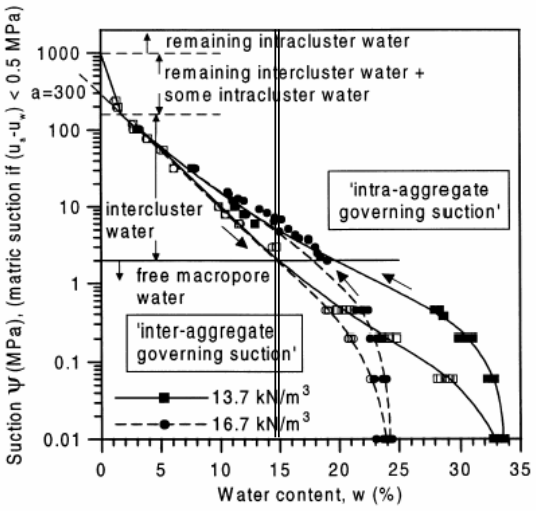

Figure 35. Main wetting and main drying retention curves at constant porosity. Intra- and inter-aggregate governing suctionzones (Romero et al. 1999)

It is interesting to observe that the separation between the region where water retention is controlled by void ratio and the region where water retention does no longer depend on void ratio is controlled by water content and not suction (Romero & Vaunat 2000). In particular, the water content of w_m=15% separating these two regions has a clear physical meaning as it represents the limit between inter-aggregate and intra-aggregate porosity.

This water content was referred to as '*microstructural'* water content by Romero & Vaunat (2000). As the water content decreases to values lower than w_m, the contours of equal suction in the compaction plane become vertical (Figure 11), indicating that pore-water is no longer present in the inter-aggregate pores and has withdrawn into the aggregates. As a change in void ratio occurs mainly at the expenses of the inter-aggregate pores, suction is significantly affected only when water is present in the inter-aggregate pore-space, i.e. when the water content w>w_m. The fact that water only occupies the intra-aggregate pore-space at w=15% is confirmed by the PSD shown in Figure 10.

Results on compacted kaolin presented by Tarantino & Tombolato (2005) essentially confirmed the findings by Romero *et al.* (1999). Figure 36 reports main wetting data for compacted Speswhite Kaolin. The degree of saturation was increased by adding water ('hydraulic' wetting) and by reducing void ratio at constant water content ('mechanical' wetting). Only compression data associated with vertical stress equal or greater than compaction vertical stress were assumed to be 'main' wetting data. Selected data presented by Tarantino & Tombolato (2005) are grouped by constant void ratio and it is apparent that void ratio affects water retention behaviour in terms of degree of saturation (Figure 36a). The lower the void ratio, the higher the air-occlusion suction. The effect of void ratio on water retention behaviour of compacted and reconstituted soils has been already observed (Vanapalli et al., 1996; Huang et al. 1998; Romero & Vaunat, 2000; Karube & Kawai, 2001; Gallipoli et al., 2003a). However, Figure 36 calls attention to another important point. The main wetting curves at constant void ratio appear to be independent of the mechanism by which the degree of saturation is increased. In fact, data associated with either 'mechanical' wetting (open symbols) or 'hydraulic' wetting (solid symbols) appear to lie on the same wetting curves at constant void ratio. Similar results were obtained for reconstituted Speswhite Kaolin and reconstituted Barcelona red clayey silt (Tarantino 2009). This implies that the term 'wetting' should be generalised and associated to an increase in degree of saturation and not only water content.

The effect of void ratio is much less pronounced if main wetting data are plotted in terms of water ratio (Figure 36b). Similarly to Romero *et al.* (1999), water retention curves in terms of water ratio e_w tend to converge at high suctions. However, it is very interesting to note that the convergence occurs when the water retention curves for the compacted specimens approach the main wetting water retention curve for the same soil in reconstituted state (data from Tarantino 2009). This is clearly illustrated in Figure 37 where all data for compacted specimens are plotted together with the main wetting water retention curve of the reconstituted kaolin. This seems to confirm once again that the compacted soil is made of 'reconstituted' aggregates.

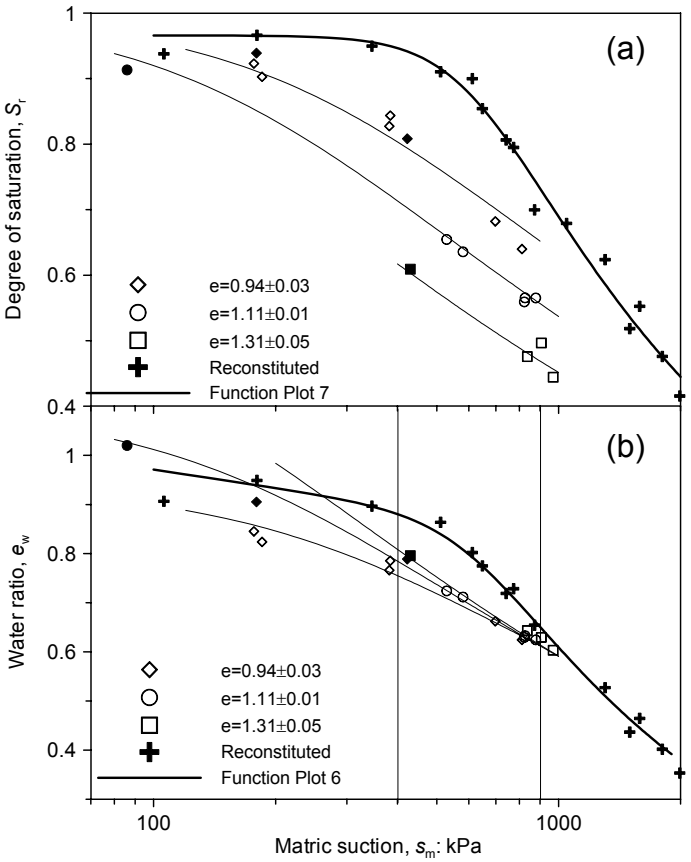

Figure 36. Selected main wetting data of compacted and reconstituted Speswhite Kaolin (solid symbols denote compacted samples wetted in a hydraulic fashion) (after Tarantino 2009).

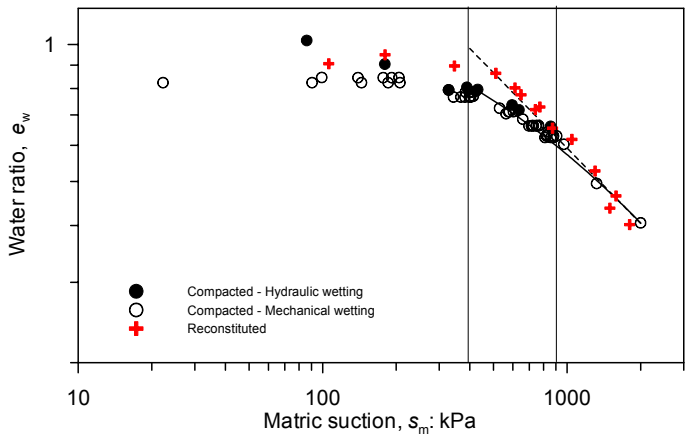

Figure 37. Main wetting data of compacted and reconstituted Speswhite Kaolin in terms of water ratio (after Tarantino 2009).

It is also worth noticing that the main wetting curves starts to deviate from the curve for the reconstituted soil at around 900 kPa (Figure 37). However, main wetting curves significantly depart from each other at around 400 kPa, the suction at which the degree of saturation of the reconstituted soil cease to increase upon a wetting path (Figure 36a). In other words, pore-water starts invading the inter-aggregate pore space as the 'reconstituted' aggregates become quasi-saturated.

Data on reconstituted Barcelona red clayey silt were obtained by Boso (2005). Samples were initially normally consolidated to 100, 300, 500 kPa vertical stress. A first series was air-dried from saturated condition (main drying) and a second series was first air-dried to hygroscopic condition and then wetted (main wetting). Figure 38 shows selected data grouped by constant void ratio. Again, the lower the void ratio, the higher is the air-entry suction (Figure 38a) both along the drying and the wetting path.

The effect of void ratio on the main drying and main wetting water retention curves is less pronounced when data are plotted in terms of water ratio (Figure 38b). In particular, the convergence of drying and wettin curves seems to ve controlled by water content (e_w~0.32) and not suction.

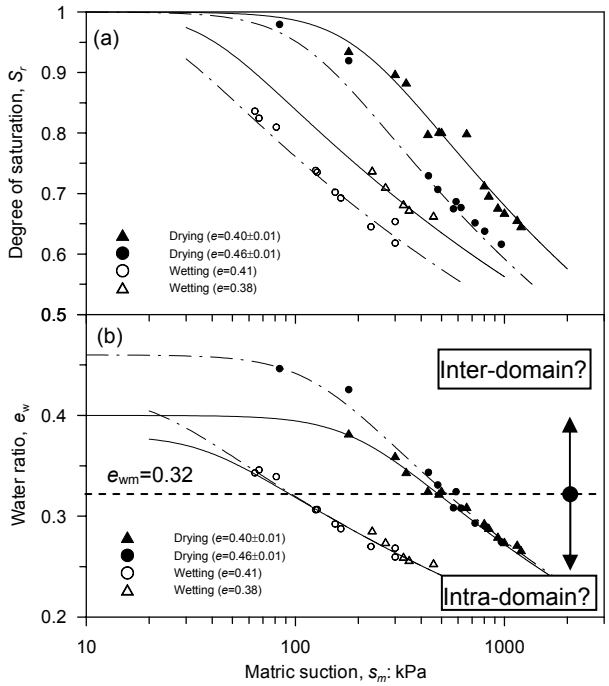

Figure 38. Selected water retention data of reconstituted red clayey silt normally consolidated to different vertical stresses (σ_{vc}=100, 300, and 500 kPa) and subsequently dried from saturated conditions or wetted from hygroscopic conditions (after Boso 2005).

The similarity between Figure 38b and Figure 35 is noteworthy. For the compacted Boom clay, the convergence of the water retention curves occurred when pore-water withdrew into the aggregates. For the case of the reconstituted Barcelona red clayey silt, it may be tentatively assumed that convergence occurred when pore-water withdrew into micro-aggregates, i.e. elementary particle assemblages. As discussed in Section 3, aggregation is present also in reconstituted soils similarly to compacted soils, the difference only lying on the size of the aggregates.

It is then interesting to compare the water retention curves of reconstituted and compacted Barcelona red clayey silt. Barrera (2002) compacted a

sample on the dry side of optimum exhibiting an initial total suction of around 2 MPa (EDO-2). This sample was subsequently placed in an axis-translation oedometer and equalised to a matric suction of 0.8 MPa. Afterwards, the sample was progressively wetted in the axis-translation oedometer. As suction was constantly decreased, the hydraulic path was therefore a main-wetting path. Buenfil (2007) compacted two samples on the dry side of optimum (with an initial suction of 270 kPa), equalised in the axis-translation oedometer at 100 kPa and then wetted until saturation and subsequently dried. Hydraulic paths investigated were therefore main wetting and main drying paths.

The comparison between compacted and reconstituted states upon wetting is shown in Figure 39a. At water ratios lower than 0.32, main wetting data from reconstituted and compacted samples superpose. The main wetting curves of the two compacted samples depart from the 'reconstituted' curve at water ratios greater than 0.32.

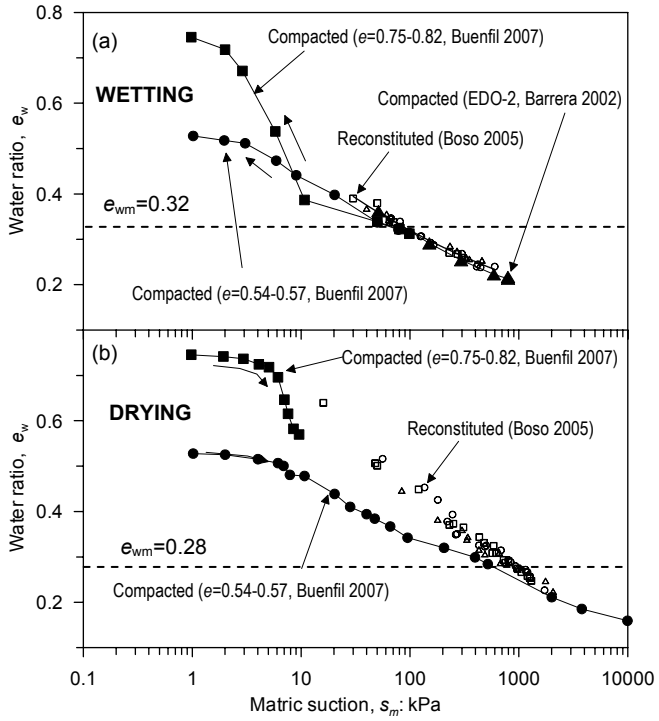

Figure 39. Main wetting and main drying data of compacted (solid symbols) and reconstituted (open symbols) red clayey silt samples (after Barrera 2002, Boso 2005, and Buenfil 2007).

Similarly, the main drying curve on compacted sample (e=0.54-0.57) tend to converge to the reconstituted curve at a slightly lower water ratio (e_w~0.28) as shown in Figure 39b. It is remarkable that convergence of 'compacted' and 'reconstituted' curves occurs at approximately the same water ratio where convergence of 'reconstituted' curves at different void ratios is observed in Figure 38. On the other hand, the effect of void ratio on the main drying curves is more significant in the compacted state (compare Figure 38b and Figure 39b).

It may be tentatively concluded that both reconstituted and compacted samples are aggregated soils, the main difference lying on the aggregate size. In the compacted samples, large aggregates produce large inter-aggregate pores, much larger than intra-aggregate pores (as evidence by the bi-modal PSD). As pore-water invades the inter-aggregate space, water retention curves significantly deviate from the curves of the 'reconstituted' aggregates (Figure 39b). On the other hand, aggregates in reconstituted soils are much smaller in size and inter-aggregate and intra-aggregate pores are of the same order of magnitude (as evidenced by the mono-modal PSD). As a result, differences in the inter-aggregate portion of the water retention curves are less significant (Figure 39b).

A comparison between water retention behaviour of soils in reconstituted and compacted states can also be made by analysing data obtained on London clay. Marinho (1994) compacted samples at different water contents and dry densities (Figure 40), which were saturated and subsequently dried. He also tested a sample reconstituted from slurry. Suction was measured using the filter paper in all tests.

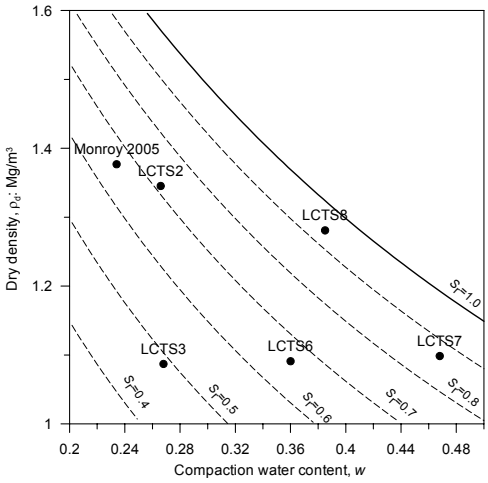

Figure 40. Samples of London Clay subjected to main drying after saturation (LCTS series) and to main wetting after compaction (after Marinho 1994 and Monroy 2005).

Main drying curves of compacted samples in terms of water ratio e_w tend to converge to the same curve as suction is increased, which also corresponds to the main drying curve of the reconstituted specimen. It is very interesting to notice that the water ratio at which the drying curves converge to the reconstituted curve depends on the compaction water content.

The specimen LCTS7 and LCTS8, compacted at the higher water contents, essentially superpose to the reconstituted main drying curve in terms of water ratio over the entire range of suction. The sample LCTS6 compacted at w=0.36 converges at suction of

around 700 kPa, the samples LCTS2 and LCTS3, were both compacted at w=0.27 and both converged at a suction of around 4000 kPa. It may be inferred that, at high water content, the compacted soil is made of very large aggregates and reduced inter-aggregate pore space (see PSD in Figure 7 and Figure 21). In such a condition, the compacted soil made of large 'reconstituted' aggregates would not significantly differ from the soil reconstituted from slurry. There is thefore no difference between the water retention curves of the reconstituted soil and the soil compacted at high water content.

As compaction water content decrease, the size of the aggregates decreases and inter-aggregate pore space increases (see PSD in Figure 7 and Figure 8). As a result, pore-water remains into the inter-aggregate voids over a wide range of suction and differences are observed between compacted and reconstituted soil until water eventually withdraws into the aggregates

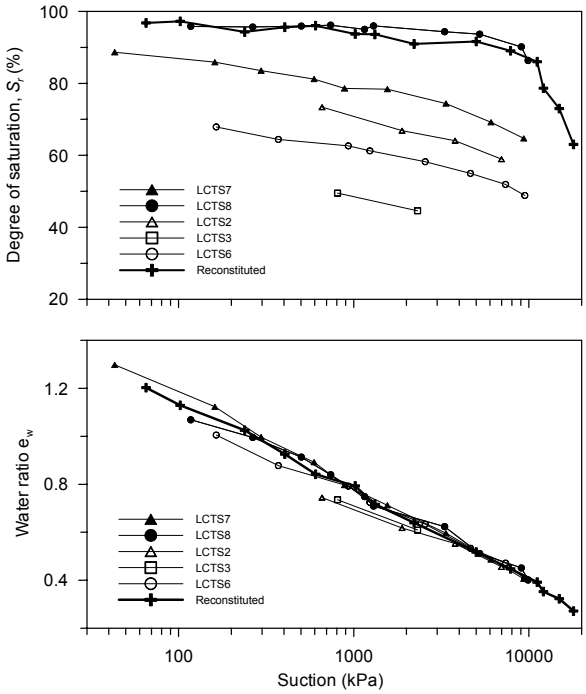

Figure 41. Water retention main drying data of reconstituted and compacted London Clay (after Marinho 1994)

For the same reason, the sample compacted by Monroy (2005) at the relatively low water content of w=0.23 (see Figure 40) and subjected to a main wetting path in the osmotic oedometer, showed a water retention curve that was affected by void ratio only at very low suctions. Figure 42 shows main wetting data obtained from oedometer tests where samples where subjected to compression at constant suction or wetting at constant vertical stress. Data shown in the figure include both 'mechanical' wetting data (degree of saturation increased mainly due to a reduction in void ratio) and 'hydraulic' wetting (degree of saturation increased mainly due to an increase in water content. In the same figure post-compaction data are also reported as a reference. It can be seen that at suction higher than 40 0kPa the water retention curve in terms of water ratio is not affected by void ratio (void ratios are given in Figure 40a). At suctions lower than around 40 kPa water ratio appear to depend on void ratio similarly to the Barcelona red clayey silt (compare with Figure 39a).

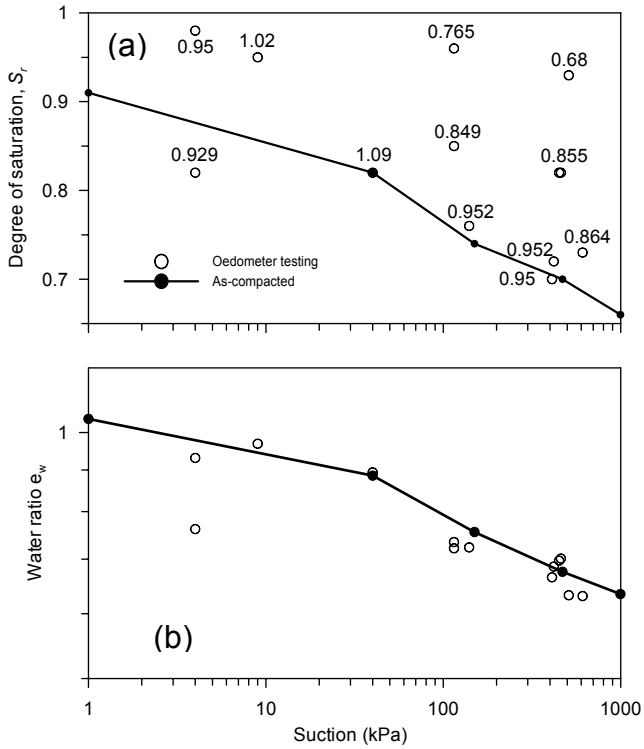

Figure 42. Main wetting water retention data of compacted London Clay (after Monroy 2005)

Finally, it is interesting to show the results from Huang *et al.* (1998) who investigated the effect of void ratio on water retention behaviour of a reconstituted silty sand including a clay fraction of only 10%. Specimens were one-dimensionally preconsolidated to different normal stresses and completely unloaded prior to being moved to the pressure-plate cells. Samples were therefore dried in pressure-plate cell. Figure 43 shows that main drying water retention curves in terms of water ratio are affected by void ratio over a significant range of suction and that these curves tend to become independent of void ratio when the degree of saturation is close to the residual value. It may be inferred that the low clay content generates little aggregation and that the water retention behaviour is dominated by capillary water in the inter-grain pore space. As a result, water retention behaviour changes significantly as the inter-grain pore space is reduced by preliminary one-dimensional compression.

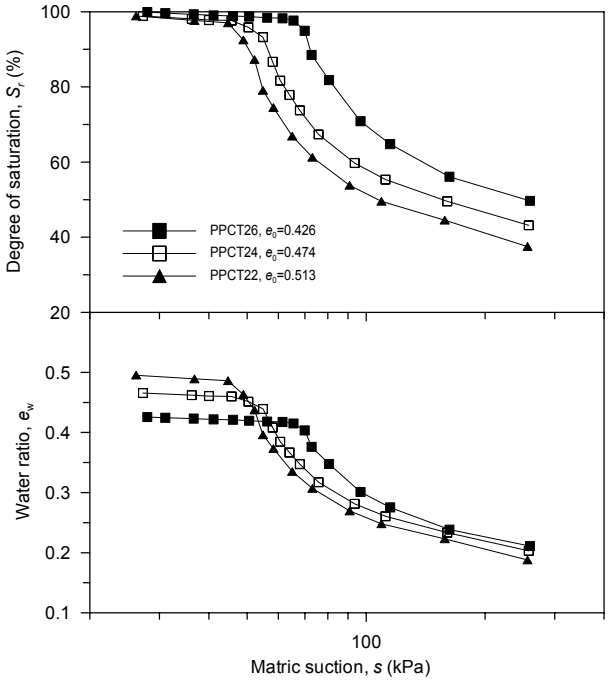

Figure 43. Main dying curves of reconstitued silty sand consolidated to different initial void ratios (after Huang et al. 1998)

8 CONCLUSIONS

The paper has presented a comparison between compacted and reconstituted states. The microstructure was first examined by analysing MIP data. It has been shown that the compaction water content plays a key role in the microfabric of the compacted soil as it controls the size of the aggregates. A simple microstructure model has been presented to explain the relationship between compaction water content and aggregation.

After compaction, soils compacted on the dry side of optimum exhibit a bi-modal pore size distribution whereas soils compacted on the wet side of optimum often exhibit (but not always) a mono-modal pore size distribution. However, mechanical and hydraulic effects can significantly modify the pore size distribution, which can evolve from mono-modal to bi-modal or vice versa. The classification of compacted soils in terms of pore size distribution (single- or double-porosity) may therefore be not always appropriate. In addition, pore size distribution may evolve significantly even when no macroscopic effects are observed as occurs when drying the compacted soils from saturated conditions.

Reconstituted soils very often exhibit a mono-modal pore size distribution even if aggregates are observed in the scanning electron microscope. Aggregates in reconstituted soils are smaller than aggregates in compacted soils and can be classified as domains or elementary particle arrangements as a first approximation. As intra- and inter-domain pores in reconstituted soils are of the same order of magnitude, it is difficult to differentiate them on the basis of the mercury intrusion porosimetry data.

When comparing the PSD of the same soil in compacted and reconstituted state, it appears that the single modal size in reconstituted soils corresponds to the intra-aggregate modal size in compacted double-porosity soil. In other words, aggregates appear to be made of 'reconstituted' soil. As in reconstituted soils, aggregates are therefore in turn formed by micro-aggregates.

Water retention behaviour appears to be directly controlled by the microstructure. In particular, water retention curves appear to be controlled by void ratio when water is present in the inter-aggregate pore space. This applies to compacted soils but it would also seem to apply to reconstituted soils. Aggregation would be present in both compacted and reconstituted soils, the difference lying on the aggregate size, macro-aggregate in compacted soils and micro-aggregate in reconstituted soils.

The comparison of the water retention curves of soils in compacted and reconstituted states then appears to confirm the 'reconstituted' nature of the aggregates.

ACKNOWLEDGMENTS

The author wishes to thank Prof. Pierre Delage, Prof. Cristina Jommi, Dr. Azad Koliji, Dr. Enrique Romero, Dr. Andrew Ridley, and Prof. Paul Simms for the helpful discussions. He also wishes to thank Grainne McCloskey for kindly reviewing the manuscript and the helpful suggestions.

REFERENCES

Ahmed, S., Lovell, C.W. Jr. & Diamond, S. 1974. Pore size and strength of compacted clay. *Journal of the Geotechnical Engineering Division, ASCE,* 100 (4): 407-425.

Alonso, E. E., Gens, A. & Josa, A. 1990. A constitutive model for partly saturated soils. Ge´otechnique 40 (3): 405–430.

Alonso, E.E., Gens, A. & Hight, D.W. 1987. Special problems soils. General report. *Proc. 9th Europ. Conf. Soil Mech. Found. Eng.*, Dublin, 3: 1087-1146.

Banin, A. & Amiel, A. 1970. A correlative study of the chemical and physical properties of a group of natural soils in Israel. *Geoderma*, 3: 185-198.

Barrera, M 2002. *Estudio experimental del comportamiento hidro-mecánico de suelos colapsables*. PhD Thesis, Universidad Polite´cnica de Catalunya, Barcelona, Spain.

Boso, M. 2005. *Shear strength behaviour of a reconstituted partially saturated clayey silt*. PhD dissertation, Università degli Studi di Trento, Italy.

Buenfil C.M. 2007. *Caracterización experimental del comportamiento hidromecánico de una arcilla compactada*. PhD Thesis, Universidad Polite´cnica de Catalunya, Barcelona, Spain.

Carter M.R. 2004. Researching structural complexity in agricultural soils. *Soil & Tillage Research* 79: 1–6.

Christenson, H. K. 1994. Capillary condensation due to van der Waals attraction in wet slits. *Phys. Rev. Lett*., 73(13): 1821–1824.

Collins, K. & McGown, A. 1974. The form and function of microfabric features in a variety of natural soils. *Géotechnique*, 24: 233-254.

Cui Y.J. 1993. *Etude du comportement d'un limon compacté non saturé et sa modélisation dans un cadre élasto-plastique*. PhD Thesis, CERMES-ENPC, Paris, France.

Cui, Y. J. & Delage, P. 1996. Yielding and plastic behaviour of an unsaturated compacted silt. *Géotechnique* 46 (2): 291–311.

Cuisinier, O. & Laloui, L. 2004. Fabric evolution during hydromecanical loading of a compacted silt. Int. J. Numer. Anal. Meth. Geomech. 28(6): 483–499.

Delage P: 2009. Discussion: Compaction behaviour of clay. *Géotechnique* 59(1): 75–77.

Delage, P. & Graham, J, 1995. Mechanical behaviour of unsaturated soils: Understanding the behaviour of unsaturated soils requires reliable conceptual models. Unsaturated Soils. Proc. 1st Int. Conf. on Unsaturated Soils (UNSAT 95), Paris, France (ed. Alonso, E.E. and Delage, P.), Rotterdam: Balkema, 3: 1223-1256.

Delage, P. & Pellerin, F. M. 1984. Influence de la lyophilisation sur la structure d'une argile sensible di Quèbec. *Clay Miner.* 19(2): 151–160.

Delage, P. & Lefebvre, G. 1984. Study of the structure of a sensitive Champlain clay and of its evolution during consolidation. *Can. Geotech. J.* 21(1): 21–35.

Delage, P. 2010. A microstructure approach to the sensitivity and compressibility of some Eastern Canada sensitive clays. *Géotechnique* 60(5): 353–368.

Delage, P., Audiguier, M., Cui, Y.J. & Howat, M.D., 1996. Microstructure of a compacted silt. *Canadian Geotechnical Journal*, 33: 150-158.

Delage, P., Marcial, D., Cui, Y. J. & Ruiz, X. 2006. Ageing effects in a compacted bentonite: a microstructure approach. *Géotechnique* 56 (5): 291–304.

Delage, P., Tessier, D. & Marcel-Audiguier, M. 1982. Use of the Cryoscan apparatus for observation of freeze-fractured planes of a sensitive Quebec clay in scanning electron microscopy. *Can. Geotech. J.* 19(1): 111–114.

Diamond, S. 1970. Pore size distributions in clay. *Clays Clay Miner.* 18: 7–23.

Diamond, S. 1971. Microstructure and pore structure of impact-compacted clays. *Clays Clay Miner*, 19: 239-249.

Dirksen C and Dasberg S 1993. Improved calibration of time domain reflectometry soil water content measurements. Soil *Sci. Soc. Am. J*., 57::660–667.

Gallipoli, D., Gens, A., Sharma, R. & Vaunat, J. 2003a. An elasto-plastic model for unsaturated soil incorporating the effects of suction and degree of saturation on mechanical behaviour. *Géotechnique* 53, No. 1, 123–136.

Gallipoli, D., Wheeler, S. J. & Karstunen, M. 2003b. Modelling the variation of degree of saturation in a deformable unsaturated soil. *Géotechnique* 53(1): 105–112.

Galvani, A. 2003. *Resistenza a taglio di un argilla non satura ricostituita in laboratorio*. Laurea Thesis, Universita` degli Studi di Trento, Italy.

Garcia-Bengochea, I., Lovell, C.W., Altschaeffl, A.G., 1979. Pore distribution and permeability of silty clays *Journal of the Geotechnical Engineering Division, ASCE* 105 (7): 839–856.

Gens, A., Alonso, E. E., Suriol, J. & Lloret, A. 1995. Effect of structure on the volumetric behaviour of a compacted soil. *Proc. 1st Int. Conf. on Unsaturated Soils*, Paris 1, 83–88.

Gomez R., Romero E., Lloret A., & Suriol J. 2009. Characterising the collapsible response of an in-situ compacted silt. In Proc. of 4th Asia Pacific Conference on Unsaturated Soils (O. Buzzi, S. Fityus & D. Sheng, eds.), CRC Press: 371-376.

Griffiths, F.J. & Joshi, R.C. 1989. Change in pore size distribution due to consolidation of clays. *Géotechnique*, 39(1): 159-167.

Hattab, M., Bouziri-Adrouche, S. and Fleureau, J-M 2010. Évolution de la microtexture d'une matrice kaolinitique sur chemin triaxial axisymétrique. *Can. Geotech*. J. 47(1): 34–48.

Huang, S., Barbour, S. L. & Fredlund, D. G. 1998. Development and verification of a coefficient of permeability function for a deformable unsaturated soil. *Can. Geotech. J.* 35(4): 411– 425.

Iwamatsu, M., & Horii, K. 1996. Capillary condensation and adhesion of two wetter surfaces. *J. Colloid Interface Sci*., 182: 400– 406.

Jommi, C., & Sciotti, A. 2003. A study of the microstructure to assess the relaiability of laboratory compacted soils as reference material for earth constructions. *System-based Vision for Strategic and Creative Design,* Bontempi, F. (ed.), 3: 2409-2415. Rotterdam : A. A. Balkema.

Jotisankasa, A. 2005. *Collapse behaviour of a compacted silty clay*. PhD thesis, Imperial College London.

Jotisankasa, A., Coop, M. & Ridley, A. 2009. The mechanical behaviour of an unsaturated compacted silty clay *Géotechnique* 59(5): 415–428

Karube, D. & Kawai, K. 2001. The role of pore water in the mechanical behaviour of unsaturated soils. *Geotechnical and Geological Engineering* 19: 211-241.

Koliji A. 2008. *Mechanical behaviour of unsaturated aggregated soils*. Ph.D. Thesis, No. 4011, Ecole Polytechnique Fèdèrale de Lausanne, Switzerland. .

Koliji, A., Vulliet, L. & Laloui, L 2010. Structural characterisation of unsaturated aggregated soils. Can. Geotech. J. 47: 297-311.

Li, Z.M. 1995 Compressibility and Collapsibility of Compacted Unsaturated Loessial Soils, Unsaturated Soils. Proc. 1st Int. Conf. on Unsaturated Soils (UNSAT 95), Paris, France (ed. Alonso, E.E. and Delage, P.), Rotterdam: Balkema, 1: 139-144.

Lloret, A., Villar, M. V., Sanchez, M., Gens, A., Pintado, X. & Alonso, E. E. 2003. Mechanical behaviour of heavily compacted bentonite under high suction changes. *Géotechnique* 53 (1): 27–40.

Marinho, F.A.M., 1994. *Shrinkage behaviour of some plastic soils*. PhD thesis, University of London (Imperial College), London, UK.

Monroy, R. 2006. *The influence of load and suction changes on the volumetric behaviour of compacted London Clay*. PhD thesis, Imperial College, London.

Monroy, R., Zdravkovic, L & Ridley, A. 2010. Evolution of microstructure in compacted London Clay during wetting and loading. *Géotechnique* 60(2): 105-119.

Ninjgarav, E., Chung, S-G., ;Jang, W-Y., Ryu, C-K. 2007. Pore Size Distribution of Pusan Clay Measured by Mercury Intrusion Porosimetry. *KSCE Journal of Civil Engineering* 11(3): 133-139.

Prapaharan S, White DM, Altschaeffl AG 1991. Fabric of field- and laboratory-compacted clay. *J Geotech Eng A*SCE 117(12):1934–1940.

Prapaharan, S., White, D.M., & Altschaeffl, A.G. 1991. Fabric of field- and laboratory-compacted clay. *Journal of Geotechnical Engineering, ASCE*, 117(12): 1934-1940.

Ridley, A.M. 1993. *The measurement of soil moisture suction.* Ph.D. Thesis, University of London.

Romero, E. & Vaunat, J. 2000. Retention curves in deformable clays. In *Experimental evidence and theoretical approaches in unsaturated soils* (eds A. Tarantino and C. Mancuso), pp. 91– 106. Rotterdam: A.A. Balkema.

Romero, E. and Simms, P. 2008. Microstructure investigation in unsaturated soils: A review with special attention to contribution a mercury intrusion porosimetry and environmental scanning electron microscopy. *Geotech. Geol. Eng.,* 26:705-727.

Romero, E., Gens, A. & Lloret, A., 1999. Water permeability, water retention and microstructure of unsaturated compacted Boom clay. *Engineering Geology*, 54: 117-127.

Salager S., El Youssoufi M. S., and Saix C. 2010. Definition and experimental determination of a soil-water retention surface. *Canadian Geotechnical Journal*, 47(6): 609-622.

Simms P.H. & Yanful EK 2001. Measurement and estimation of pore shrinkage and pore distribution in a clayey till during soil-water characteristic curve tests. Can Geotech J. 38:741–754.

Sridharan, A., Altschaeffl, A. G. & Diamond, S. 1971. Pore size distribution studies*. J. Soil Mech. Found. Div., ASCE* 97, 771–787.

Tamagnini, R. 2004. An extended Cam-clay model for unsaturated soils with hydraulic hysteresis, *Géotechnique* 54(3): 223–228.

Tanaka, H., Shiwakoti, D. R., Omukai N., Rito F., Locat J.; Tanaka M. 2003. Pore size distribution of clayey soils measured by mercury intrusion porosimetry and its relation to hydraulic conductivity. *Soils and Foundations*, 43(6): 63-67.

Tang A-M & Cui Y-J 2005. Controlling suction by the vapour equilibrium technique at different temperatures and its application in determining the water retention properties of MX80 clay. Can. Geotech. J. 42: 287–296.

Tarantino, A. & De Col E. 2009. Compaction behaviour of clay: Authors' reply to discussion by P. Delage. *Géotechnique*, 59(1): 75–76.

Tarantino, A. (in prep.,a). Effects of aggregation on water retention behaviour of clayey soils. In prep.

Tarantino, A. (in prep.,b). A microstructural interpretation of Bigot's drying curve. In prep.

Tarantino, A. 2009. A water retention model for deformable soils. *Géotechnique* 59(9): 751–762.

Tarantino, A. 2010. Basic concepts in the mechanics and hydraulics of unsaturated geomaterials. New Trends in the Mechanics of Unsaturated Geomaterials Lyesse Laloui (ed.). ISTE – John Wiley & Sons.

Tarantino, A., & De Col, E. 2008. Compaction behaviour of clay. *Géotechnique* 58(3): 199–213.

Tarantino, A., and Tombolato, S. 2005. Coupling of hydraulic and mechanical behaviour in unsaturated compacted clay. *Géotechnique*, 55(4): 307-317.

Thom, R., Sivakumar, R., Sivakumar, V., Murray, E. J. & Mackinnon, P. 2007. Pore size distribution of unsaturated compacted kaolin: the initial states and final states following saturation. *Géotechnique* 57(5): 469–474.

Tuller, M., & D. Or 2005. Water films and scaling of soil characteristic curves at low water contents. *Water Resour. Res*., 41, W09403, doi:10.1029/2005WR004142.

Tuller, M., Or, D., and Dudley, L. M. 1999. Adsorption and capillary condensation in porous media: Liquid retention and interfacial configurations in angular pores. *Water Resour. Res*., 35(7): 1949–1964.

Vanapalli, S. K., Fredlund, D. G. & Pufhal, D. E. (999. The influence of soil structure and stress history on the soil-water characteristics of a compacted till. *Géotechnique* 49(2): 143–159.

Vaunat, J., Romero, E. & Jommi, C. 2000. An elastoplastic hydromechanical model for unsaturated soils. *In Experimental evidence and theoretical approaches in unsaturated soils* (eds A. Tarantino and C. Mancuso), pp. 121–138. Rotterdam: A. A. Balkema.

Wheeler, S. J. & Sivakumar, V. 1995. An elasto-plastic critical state framework for unsaturated soil. *Géotechnique* 45 (1): 35–53.

Wheeler, S. J. & Sivakumar, V. 2000. Influence of compaction procedure on the mechanical behaviour of an unsaturated compacted clay. Part 2: Shearing and constitutive modelling. *Géotechnique* 50(4): 369–376.

Wheeler, S. J., Sharma, R. S. & Buisson, M. S. R. 2003. Coupling of hydraulic hysteresis and stress–strain behaviour in unsaturated soils. *Géotechnique* 53(1) : 41–54.